Enabling Supersonic Over-land Flight Using Computational Modeling

Advanced Modeling and Simulation (AMS) Seminar Series
NASA Ames Research Center, February 2nd, 2023

Scott Neuhoff, Chase Ashby, Jeff Housman, James Koch, James Jensen, Emre Sozer, Gaetan Kenway, Jared Duensing

Motivation

- Prove the feasibility of commercial supersonic travel using low-boom aircraft concepts
  - Unacceptable sonic boom noise is the main barrier to overland supersonic flight
  - Achieve a target perceived loudness of 75dB
  - Support X-59 team in experimental flights

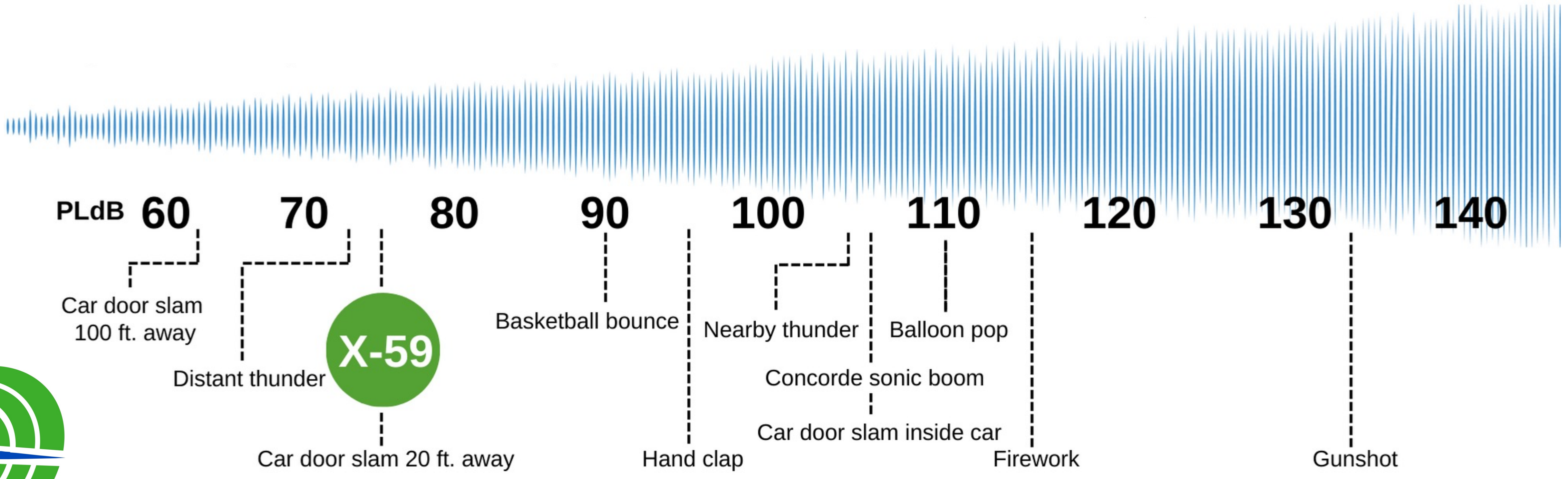

Image credit: NASA/QueSST

Motivation

Increase speed, accuracy, and robustness of near-field CFD simulations of low boom aircraft

- Improve speed of mesh generation
- Improve computational efficiency of flow solvers
- Improve the accuracy of flow solvers

Three step process:

1. Near-Field CFD
2. Mid-Field Space Marching
3. Far-Field Propagation

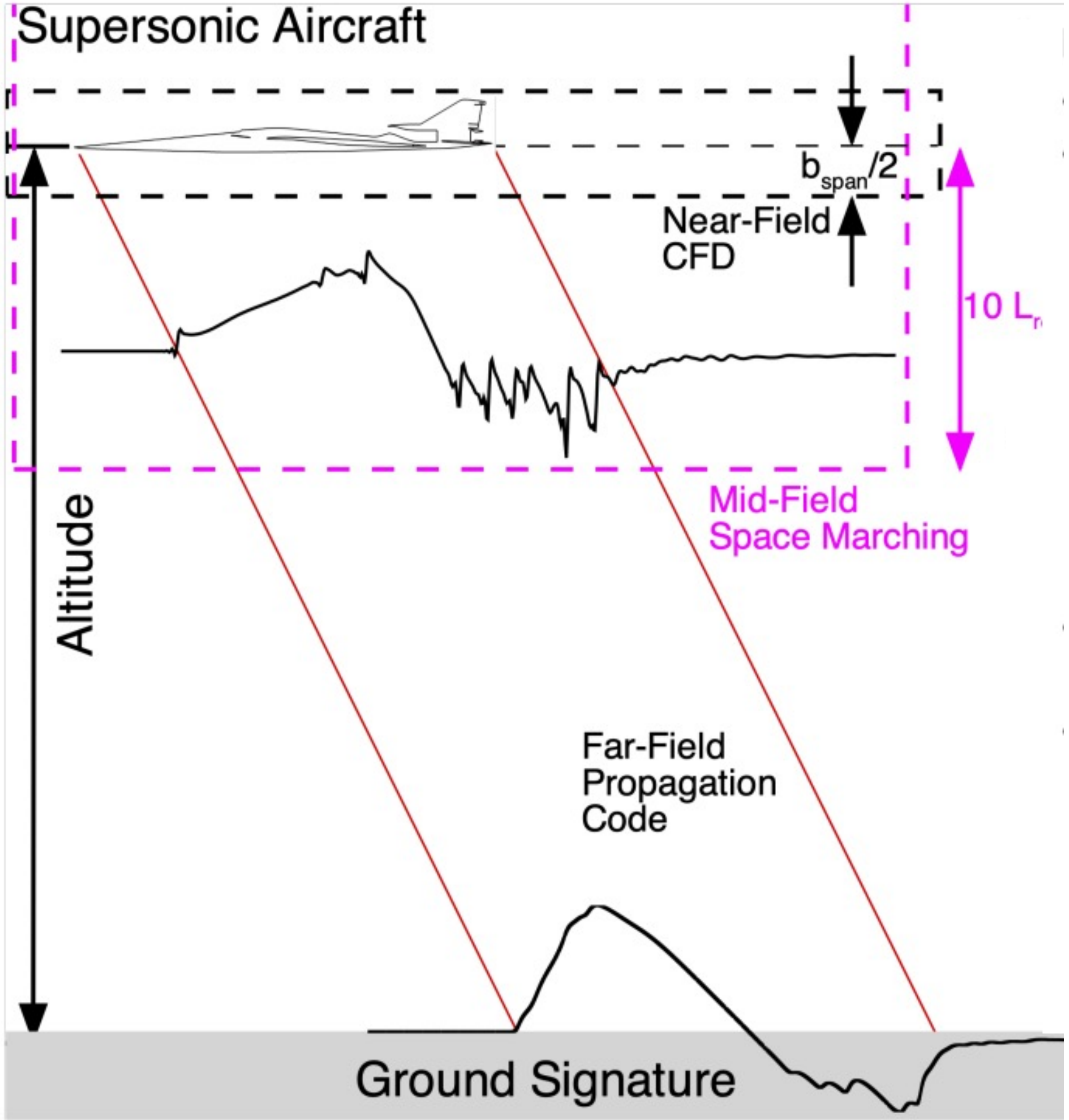

Loudness prediction procedure

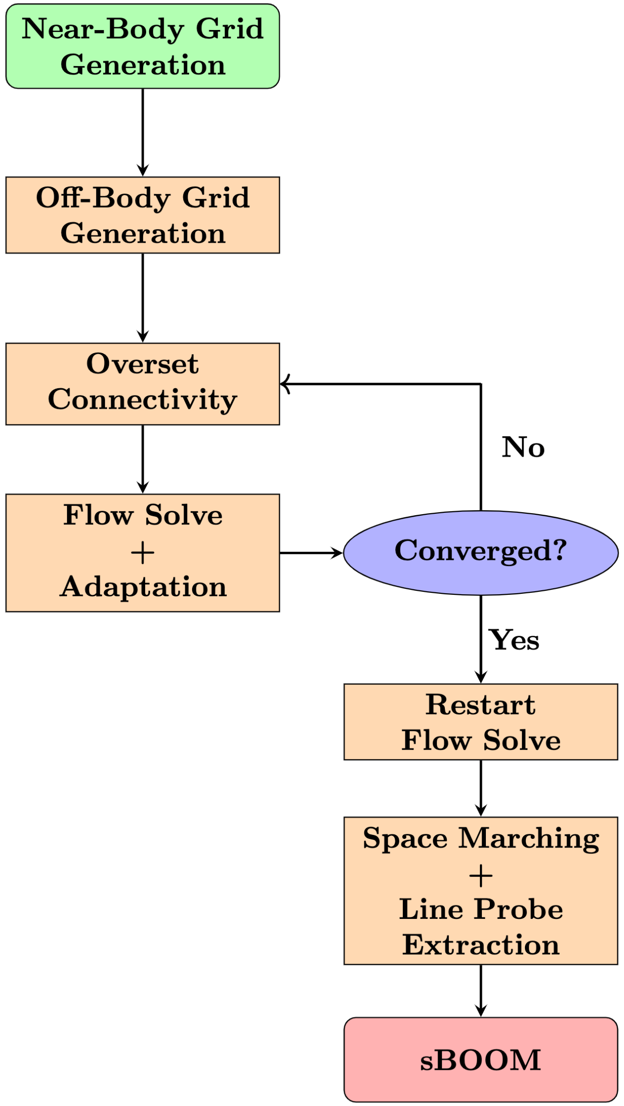

Current LAVA X-59 workflow

Mesh Paradigms within LAVA

Structured Cartesian AMR	*Unstructured Arbitrary Polyhedral*	*Structured Curvilinear*

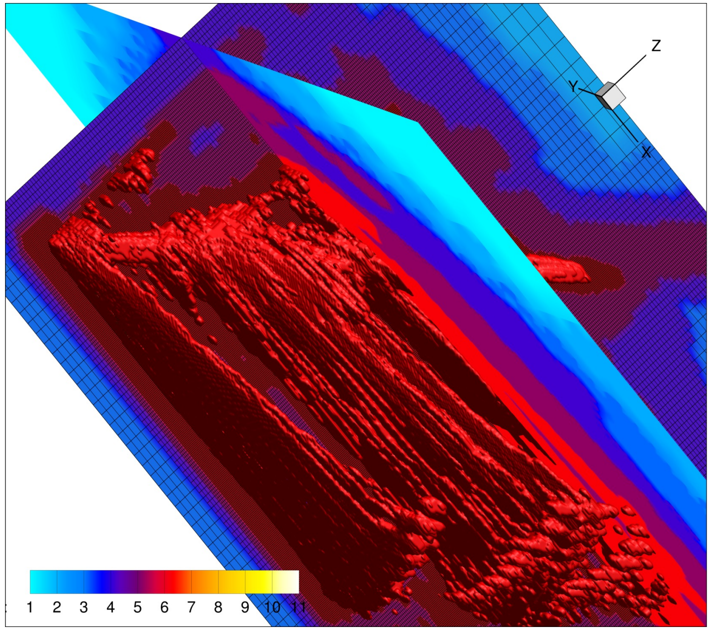

- Essentially no manual grid generation
- Highly efficient Structured Adaptive Mesh Refinement (AMR)
- Low computational cost
- Reliable higher order methods
- Non-body fitted -> Resolution of boundary layers inefficient

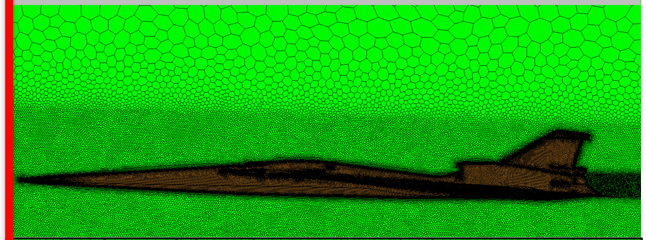

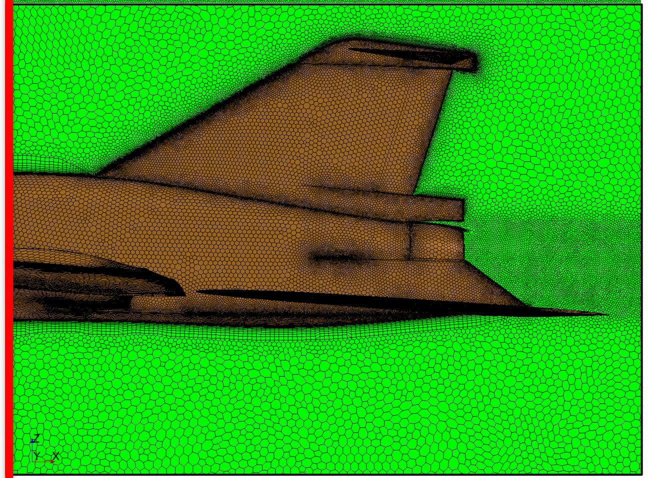

- Partially automated grid generation
- Body fitted grids
- Grid quality can be challenging
- High computational cost
- Higher order methods yet to fully mature

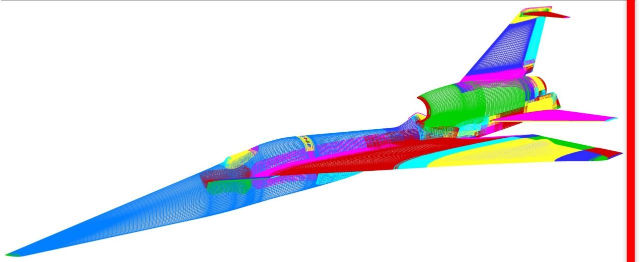

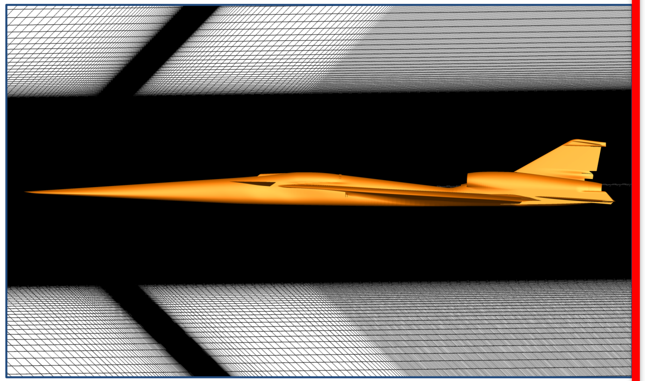

- High quality body fitted grids
- Low computational cost
- Reliable higher order methods
- Grid generation largely manual and time consuming

LAVA Framework Overview

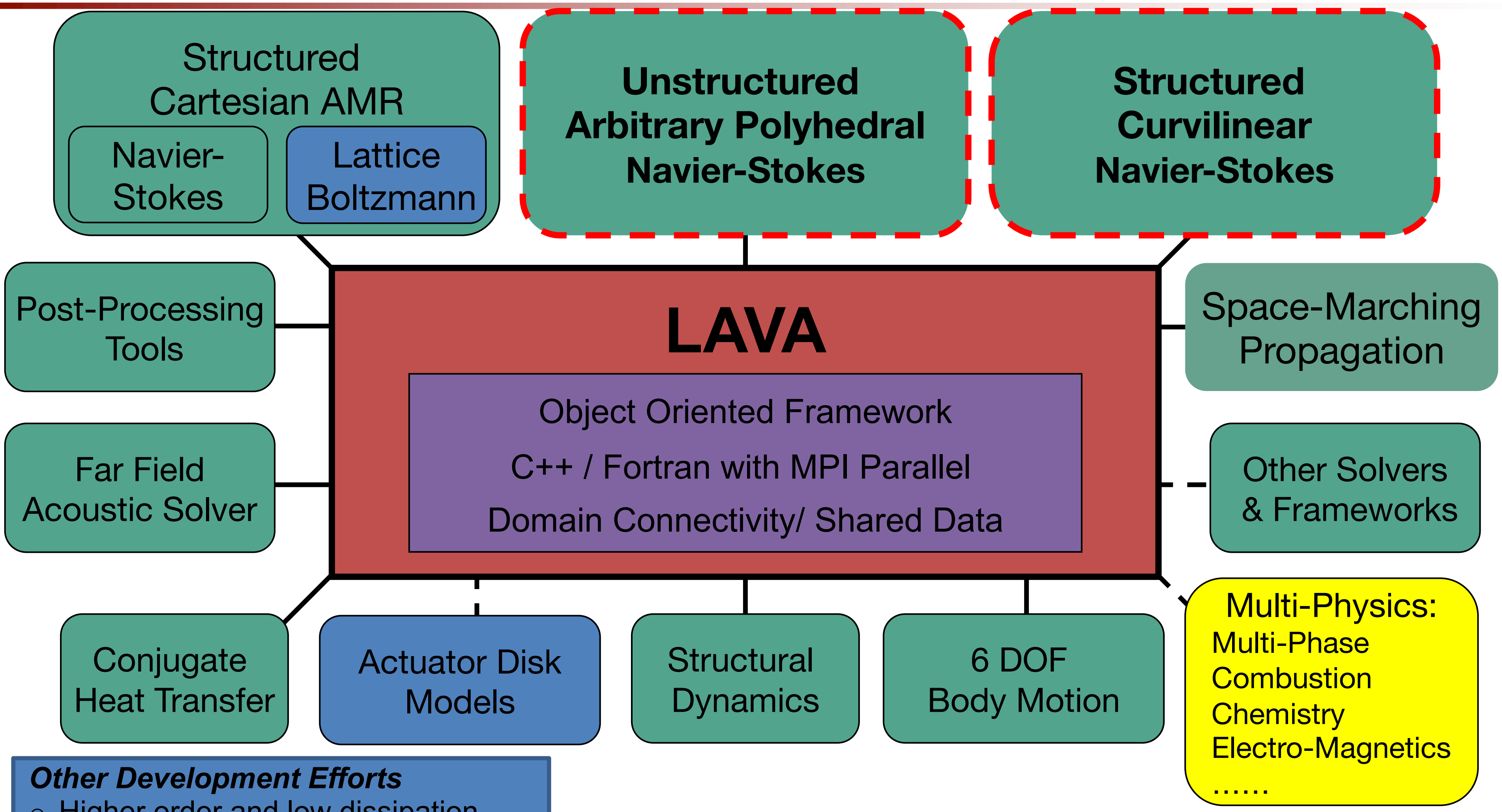

Other Development Efforts

- Higher order and low dissipation
- Curvilinear grid generation
- Wall modeling
- LES/DES/ILES Turbulence
- HEC (optimizations, accelerators, etc)

———	Connected	Existing	Developing
- - -	Not Yet Connected	Future	Framework

Kiris at al. AIAA-2014-0070 & AST-2016

Outline

- Part I
  - Space Marching
    - Solver developments
    - Improvements to usability / scripts around the solver (including line probe extraction)
  - Database automation
  - Adjoint-based mesh redistribution
    - Workflow outline
    - Example cases
  - LAVA source code developments
    - LAVA Unstructured refactor
    - Curvilinear grid generation moving from OVERFLOW hole-cutting to LAVA hole-cutting
- Part II
  - Glenn 8x6 wind tunnel comparisons
  - C608 from AIAA 3rd Sonic Boom Prediction Workshop (SBPW3)
  - Current X-59 results

Space Marching

Summary

- Added non-zero angle of attack capability to the space marching solver
- Verified Space Marching coupled to unstructured LAVA and external (non-LAVA) CFD solvers
- Developed a near-field difference propagation procedure via space marching
- Completed direct export of *Pressure Cylinder* from Space Marching for input into SBoom or PCBoom
- Improved user-friendly python driver script for better integration into the LBFD Database workflow
- Automated space marching mesh sensitivity and uncertainty quantification procedure within python driver

Significance

- Successfully coupled Space Marching to FUN3D with adapted CFD mesh and USM3D using geolab mesh on X-59 c612 configuration
- Space marching solver is being used internally within NASA
  - Coupled to LAVA structured overset grid solver and LAVA unstructured solver (J. Jensen and S. Neuhoff)
  - Coupled to FUN3D (S. Rallabhandi)
- Utilization of space marching coupled to LAVA structured overset resulted in factor of 2 savings for X-59 database generation. When combined with adaptive redistribution of the Mach-cone aligned off-body this should result in a factor of 4 reduction for same level of accuracy as standard CFD approach.

Housman, "Algorithmic Improvements to a High-Order Space Marching Method for Sonic Boom Propagation", https://www.nas.nasa.gov/pubs/ams/2022/07-21-22.html

Space Marching: Elliptic Hole Cutting Procedure

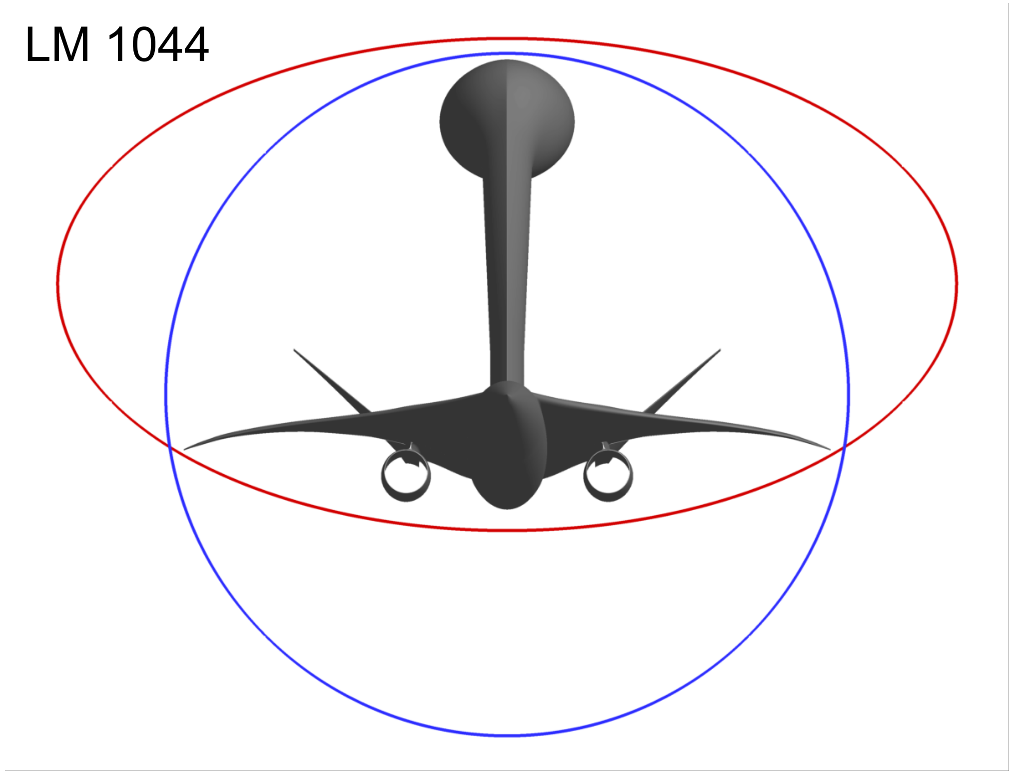

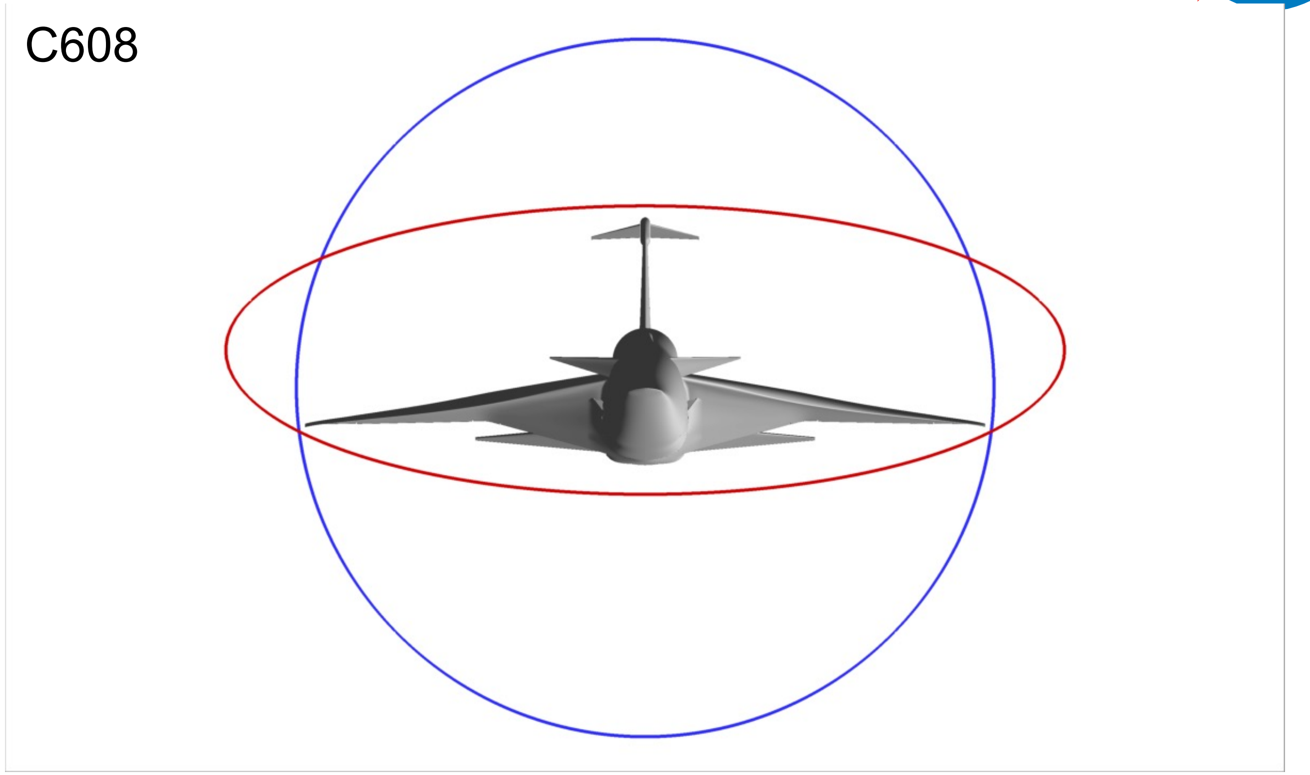

- The original cylindrical hole cutting procedure has been replaced with an elliptic hole cutting procedure
  - Remains geometrically simple for easy user placement*
  - Enables closer coupling to the aircraft
  - Reduces CFD meshing requirements away from aircraft body

*An automated multi-ellipsoidal procedure is currently being developed

Space Marching: Unstructured Solver Coupling

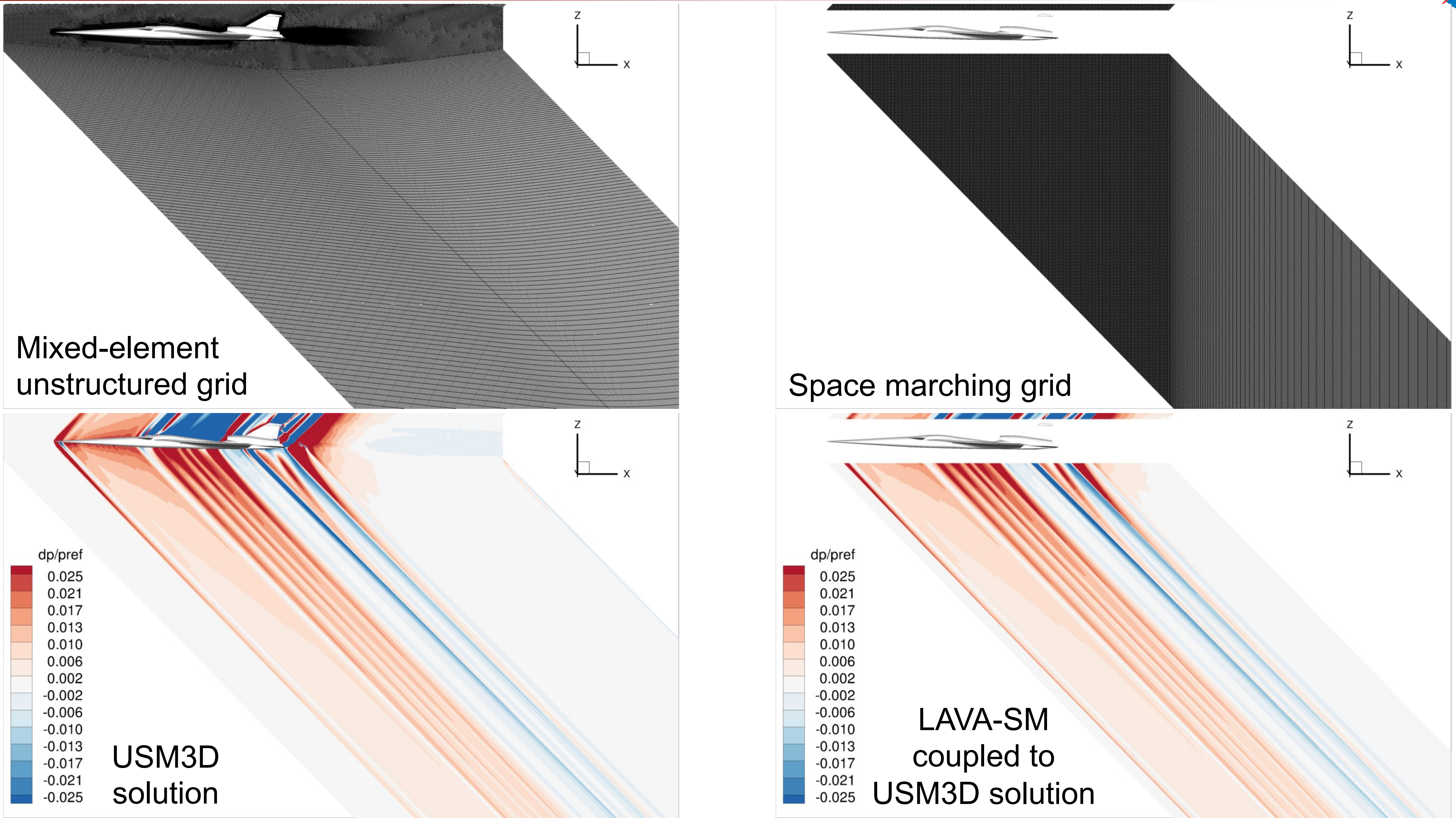

Space Marching: Unstructured Solver Coupling

- On-track comparison of pressure at r/L_{body} = 3 between USM3D and LAVA space marching coupled with USM3D using two different numerical flux options
- Both numerical schemes match USM3D very well over most of the signature
- Minor discrepancy at x/L_{body} = 3.85 reduced with higher-order scheme
- Space marching time of 138.3 and 144 seconds respectively (72 M grid points)

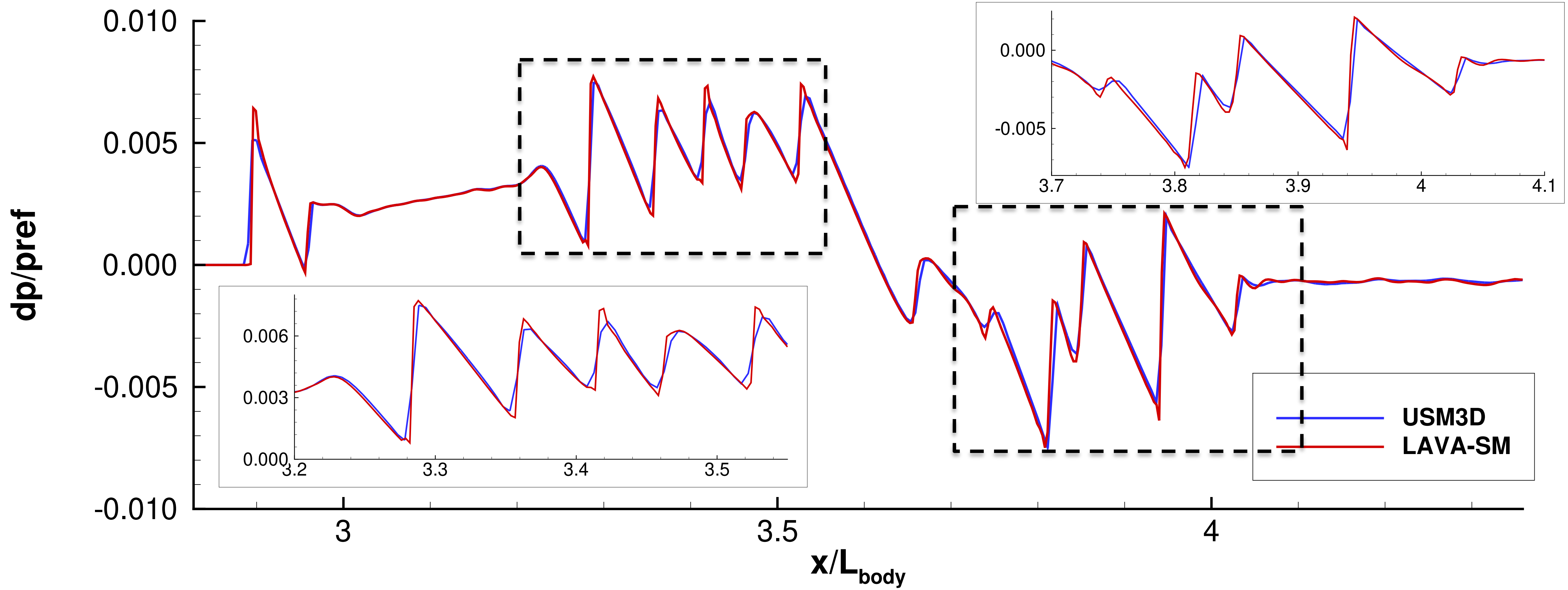

Space Marching: Accuracy Enhancement

- HALO3D solutions on the coarse, medium, and fine committee mixed-element unstructured grids were provided by the ANSYS Canada team
- A space marching mesh sensitivity study was performed using the coarse HALO3D solution
- Medium space marching grid is observed to be sufficient (72 M grid points)

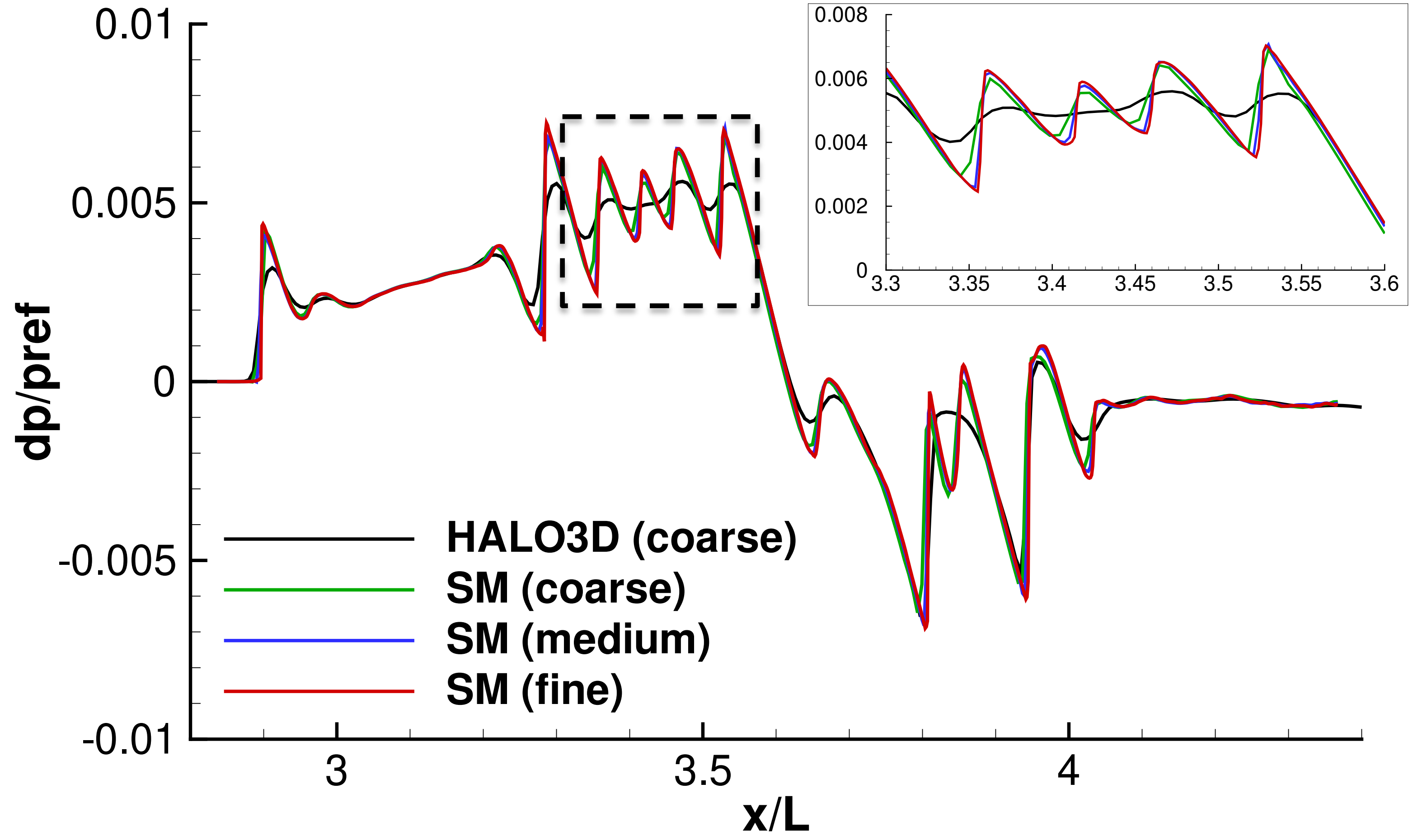

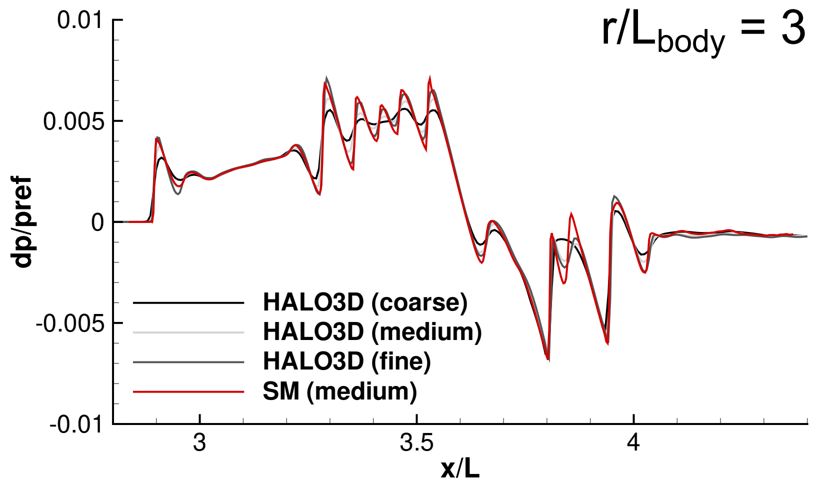

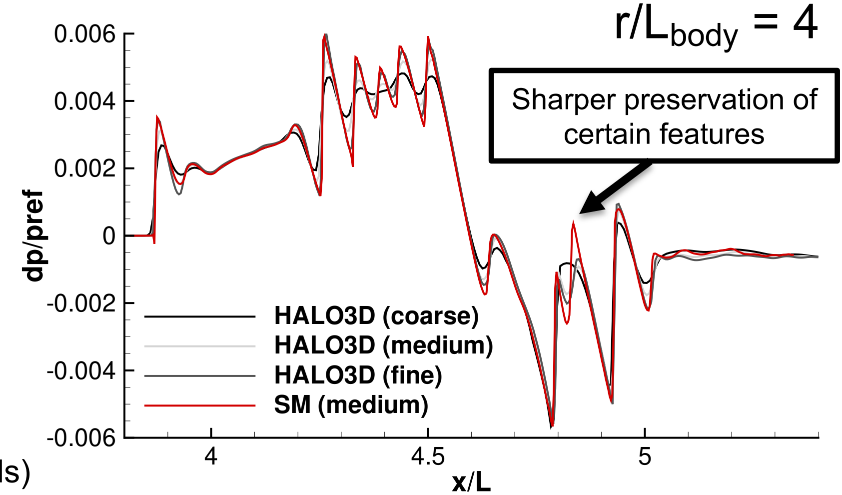

Medium grid spacing space marching improves coarse grid HALO3D solution to fine grid level (cost 2 minutes 37 seconds)

Space Marching : Near-Field Difference Propagation via Space Marching

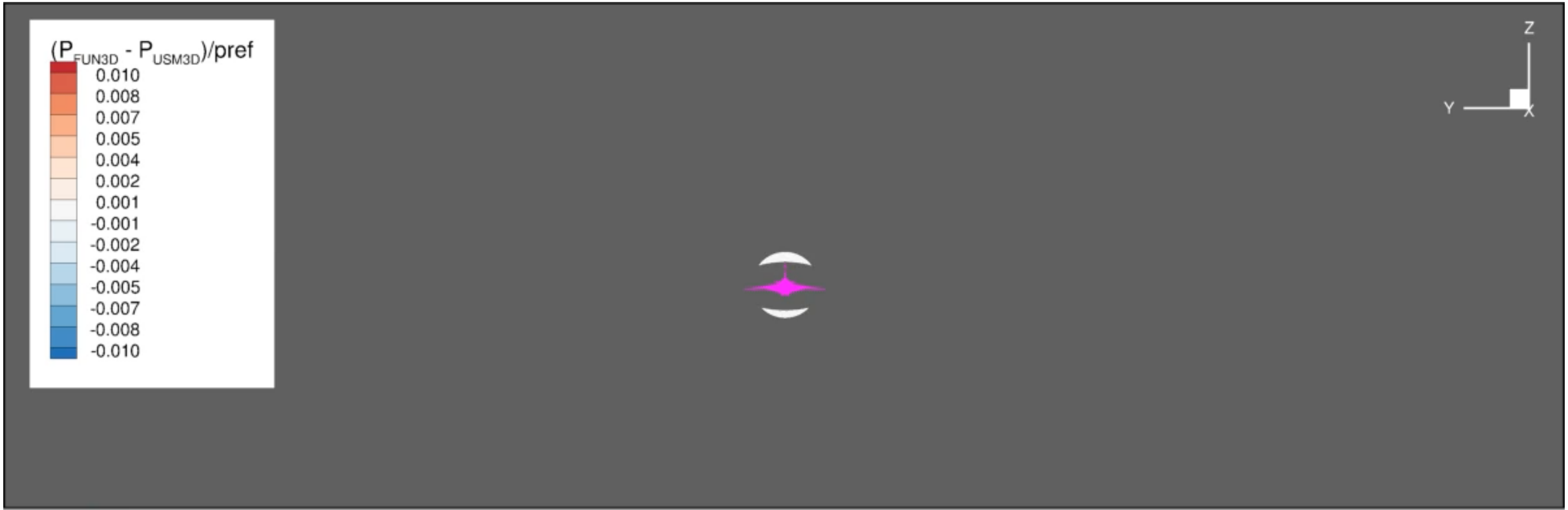

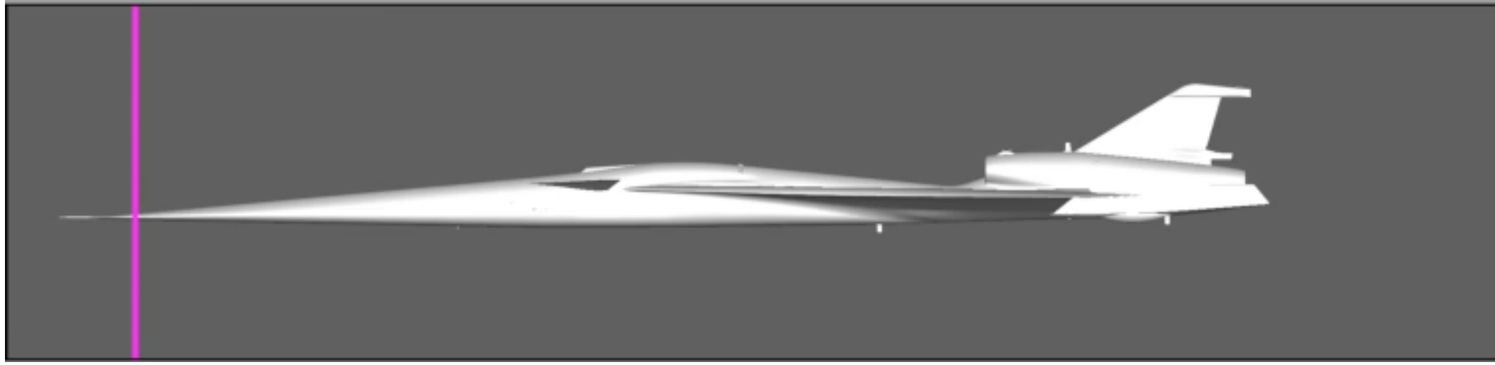

Procedure

1) Propagate FUN3D near-field using LAVA-SM
2) Propagate USM3D near-field using LAVA-SM
3) Compute difference: FUN3D+LAVA-SM – USM3D+LAVA-SM

Space Marching: Near-Field Difference Propagation via Space Marching

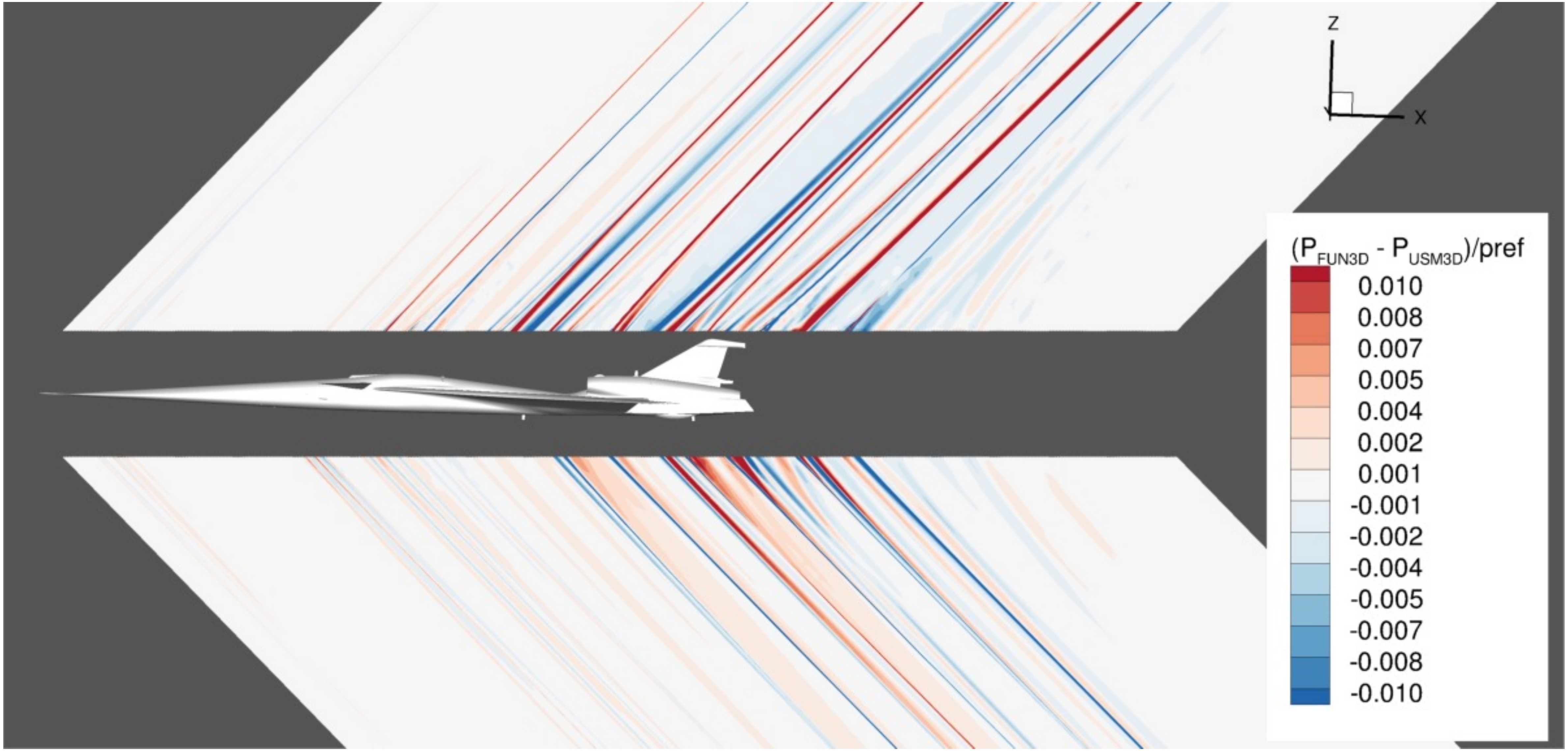

Space Marching: Improved User-friendly Python Driver

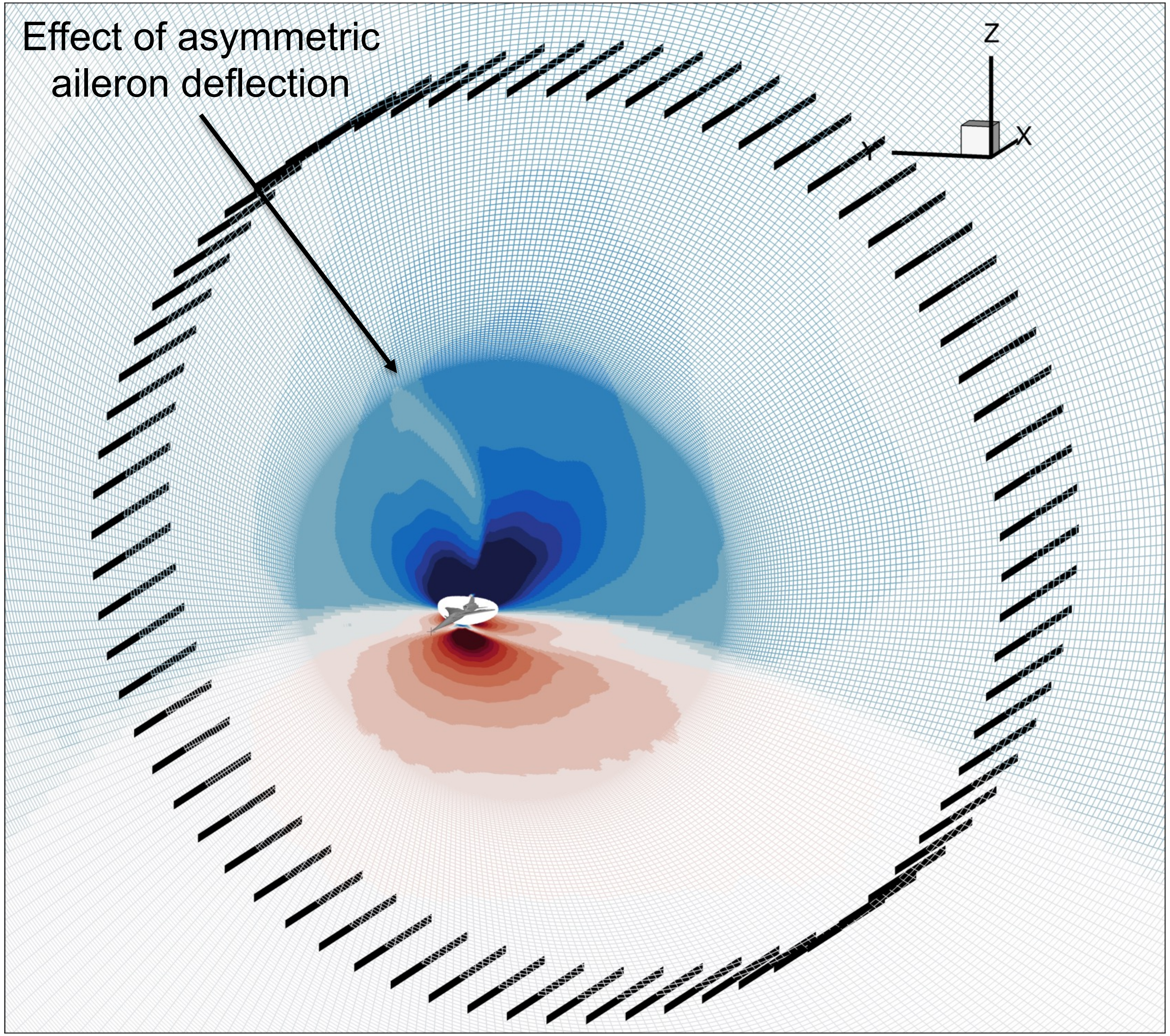

- Added user defined probe/cylinder extraction capability for coupling to far-field propagation codes
  - Reduced extract runtime from 20 minutes to 2 minutes
  - Enabled easier user specification of extraction radius
- Added user command options to perform sections of the python script
  - Grid generation and fringe point generation only
  - Entire space marching procedure
  - Entire procedure including probe/cylinder extraction for far-field propagation
  - Everything + grid sensitivity/uncertainty procedure

Database with LAVA: Running a Case with LAVA

- Physical configuration, free stream conditions, and propulsion conditions are used to generate each case's mesh
- Once the mesh is generated it is run through LAVA's implicit hole cutting
- The case is then submitted to the queue using an 8 hour job on 400 cpus
  - During this job the LAVA flow solver and space marching solvers are run
  - Convergence is typically achieved in 5-6 hours depending on node type
  - Space Marching and line probe extraction are automatically run once near-field is converged, taking less than 20 minutes wall time
- The volume and pressure cylinder output data are then checked manually for their validity

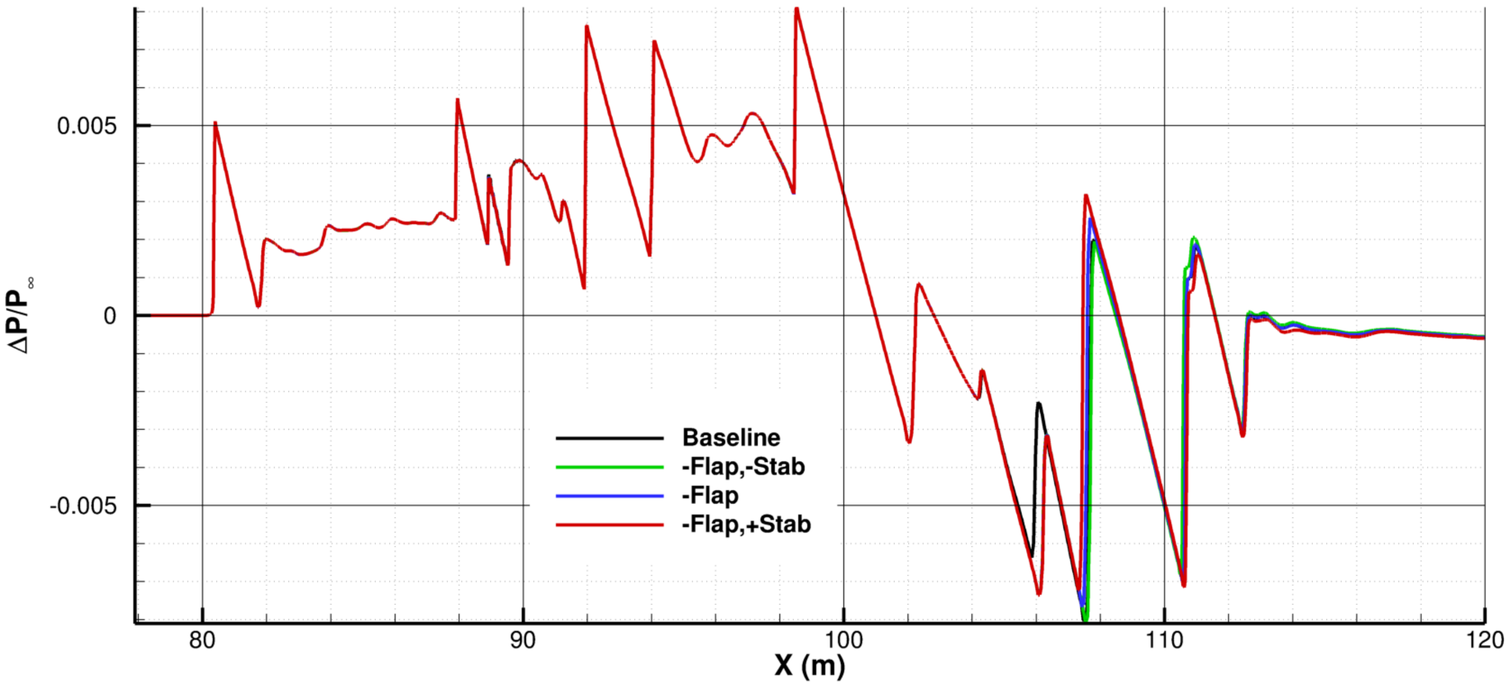

Negative Flap Deflection Example from Preliminary Database

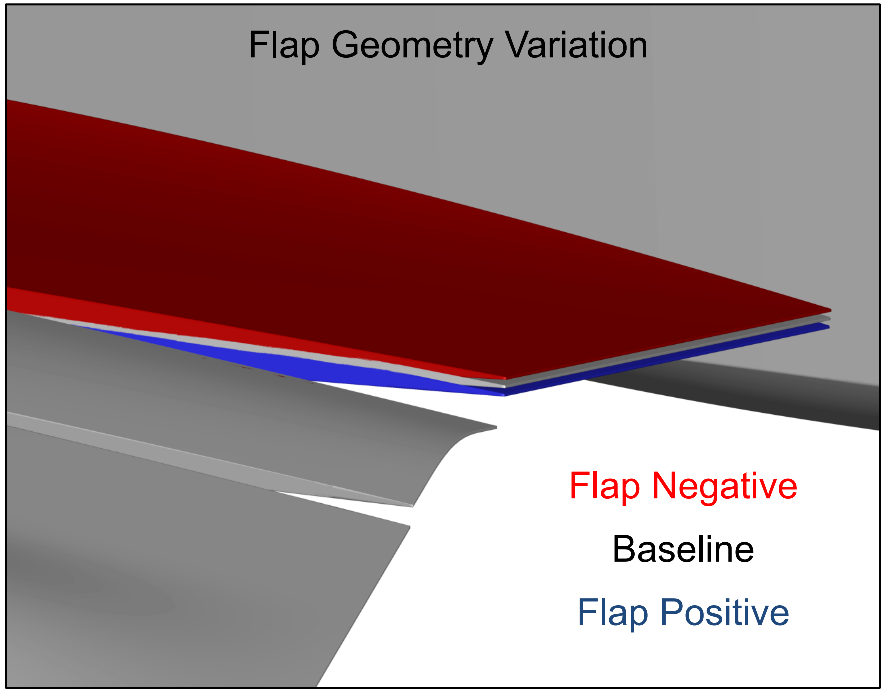

Developing Automated Tools for X-59 Database Processing in LAVA

- Automating the Process
  - Trimmed flight conditions provided by 6dof model
  - Developed a Python wrapper for building and submitting cases
  - Added the ability to automatically run the space marching code once the near field run is completed within one pbs script
  - Added the ability to directly extract pressure cylinders from the space marching code without additional user input
  - A single case can now be meshed, run, and post-processed within 8 hours (not including queue time)
- Example Workflow for Latest Database (90 Cases)
  - Convert database case spreadsheet into a CSV file (5 minutes)
  - Run the mesh building pre-processing Python script (~15mins per case, 22 hours total)
  - Submit the cases to the queue using a "shotgun" method (1 minute)
  - Run the nearfield code (5-6 hours per case)
  - Run the space marching code and output the cylinder data (20mins per case, can be run concurrently)
  - Download and verify the validity of the cylinder data once the case has finished running (2 minutes for download, varying amount of time to manually inspect the signatures)
  - Total time to produce 90 case database: 1-2 weeks
- Cost savings estimate **per case**
  - Time saved by automated build script: 10 minutes
  - Time saved by automated submission script: 10 minutes
  - Time saved by using space marching: 2 hours
  - Time saved by integrated cylinder extraction: 20 minutes
  - Total savings per case: 2 hours and 40 minutes

Database with LAVA: Extending X-59 Grid Generation Functionality

- Developed a custom procedure for dynamically generating the nozzle based on the engine setting (PLA)
  - Engine conditions from the NPSS model for the engine are extracted
  - The new internal and external nozzle outer mold line is dynamically generated using input throat area (A8) and exit area (A9)
  - Outer surface is currently approximated by a straight line; original baseline geometry is curved
  - The contour line is then revolved to create a reference surface
  - Baseline nozzle grids are then projected onto the new reference surface or dynamically generated on the new surface
- Implemented asymmetric aileron deflections
- Implemented non-zero rudder deflection

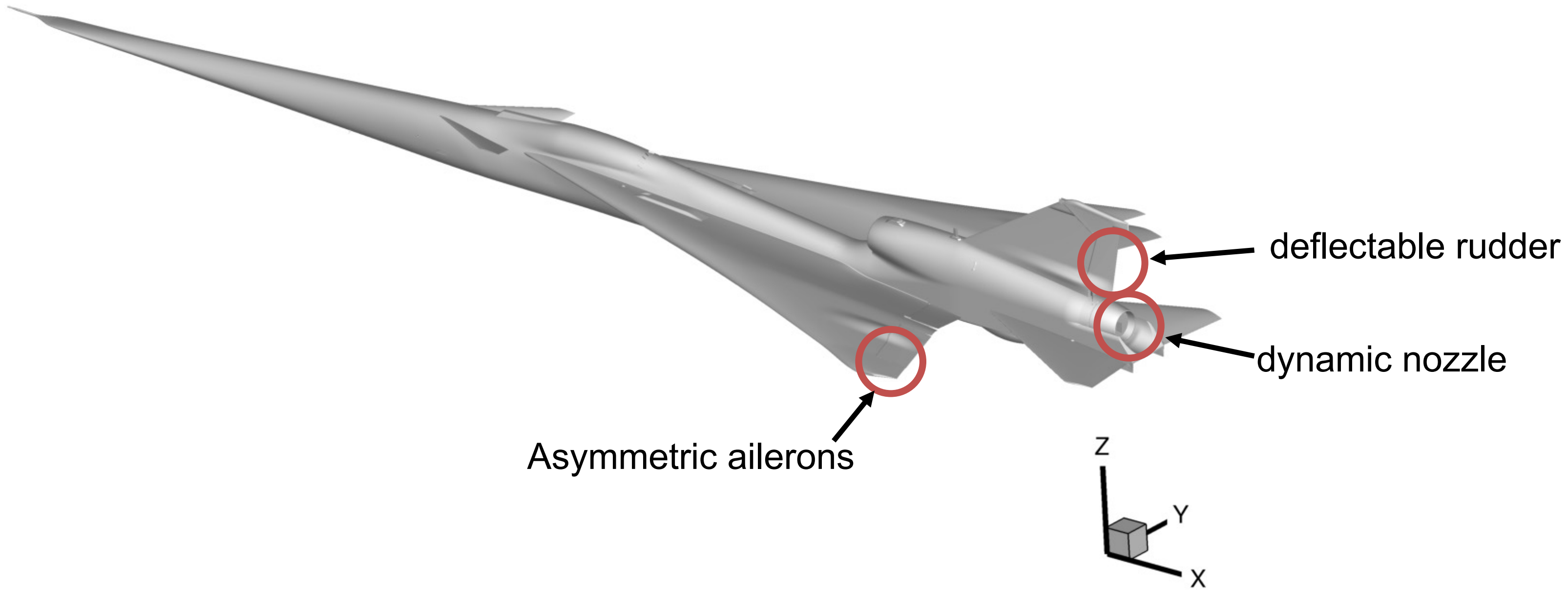

X-59 database grid generation improvements

Adjoint Method for Grid Adaptation and Design Optimization in LAVA

Recent Developments

- Implemented 1st and 2nd order LAVA adjoint solvers for design optimization
- Developed an automatic adjoint-based Mach-cone aligned off-body adaptation capability optimized for coupling with LAVA space marching
- Demonstrated ability to improve near-field and ground-level pressure signatures with half the resource requirement on the JAXA Wing Body from the 2nd AIAA Sonic Boom Prediction Workshop
- Matured capabilities on X-59 wind tunnel model and X-59 flight model

Significance

- Design tool allows for fixed cost RANS based solution evaluation and associated error estimate procedure
- Utilization of adaptive redistribution of the Mach-cone aligned off-body grid coupled with space marching should result in a factor of 4 savings for LBFD database generation with the same level of accuracy as a standard CFD approach

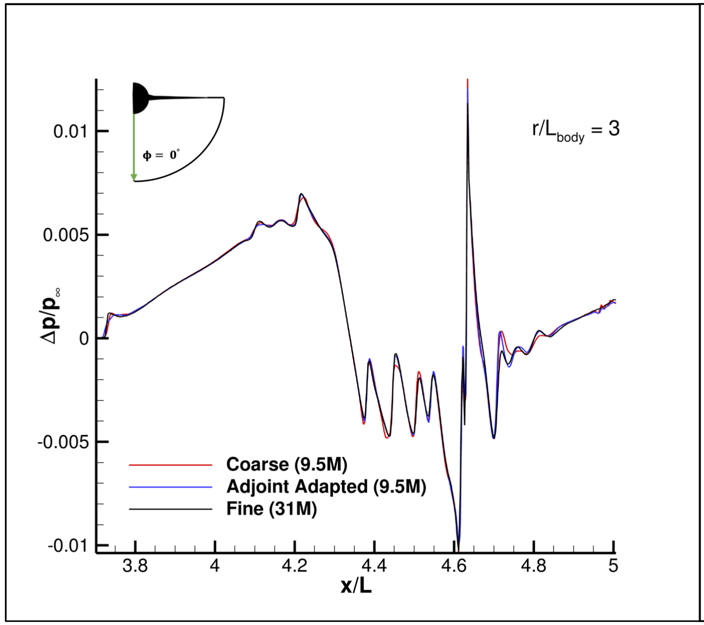

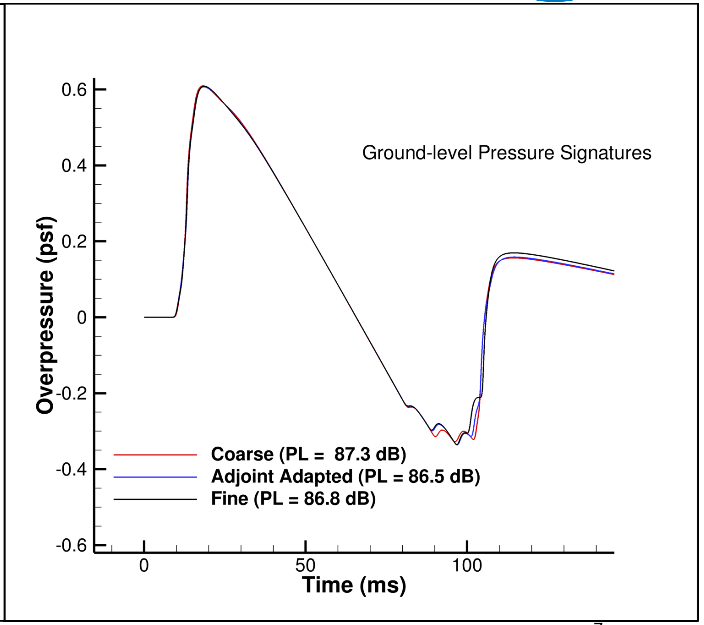

LAVA adjoint based adaptation + space marching enables 4x speedup in turnaround with same level of sonic boom prediction accuracy

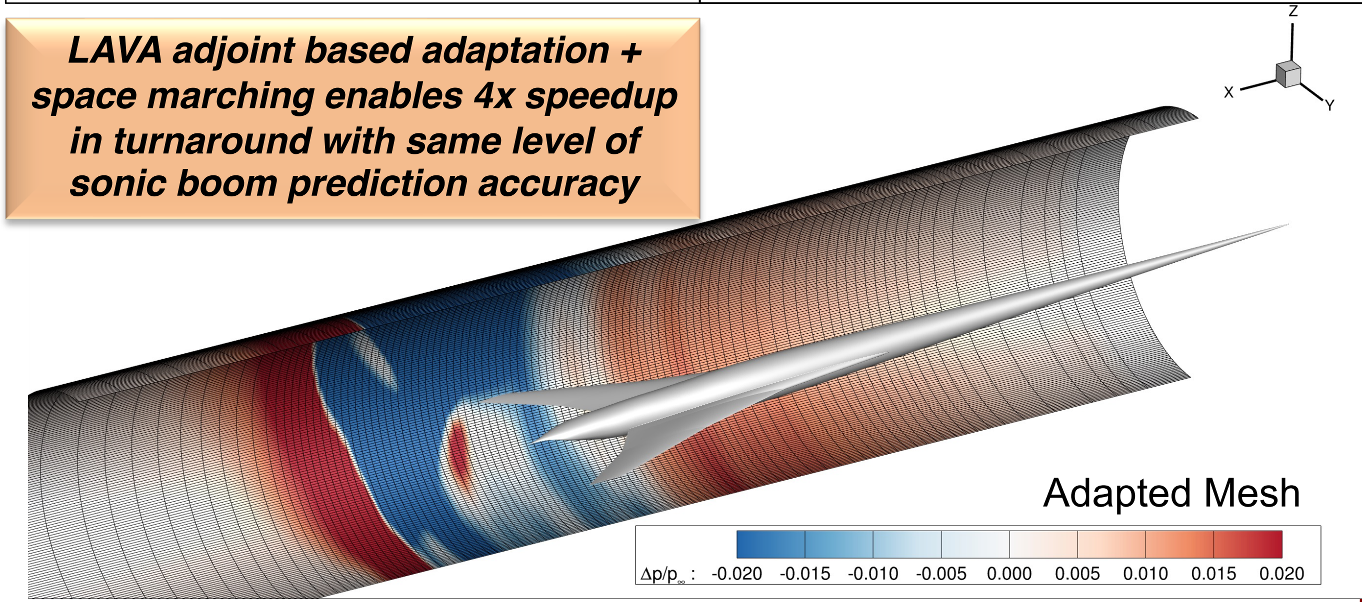

Grid Adaptation: Off-body Procedure

- Mach-cone aligned adaptation steps:

  1. **Initial off-body grid is generated with uniform streamwise and circumferential spacing**
  2. Solve governing flow equations
  3. Solve adjoint linear system
  4. **Adaptation indicator is computed, and the off-body grid is redistributed**
  5. Flow solver is restarted and converged

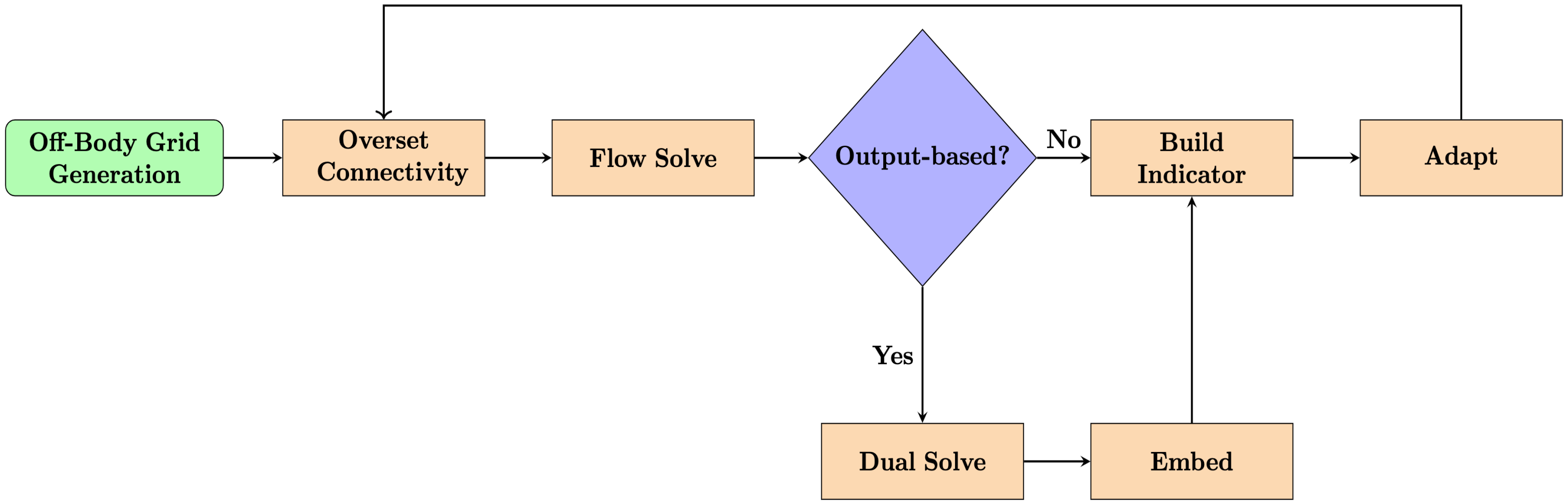

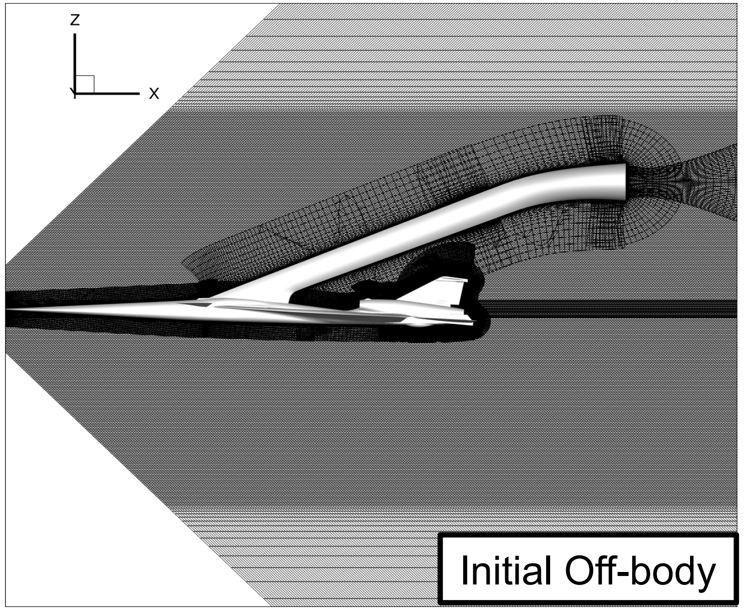

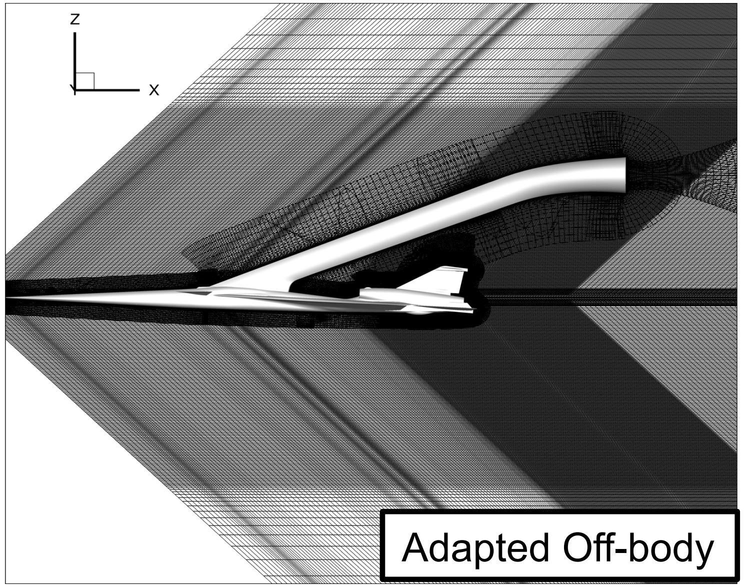

Grid Adaptation: Off-body Procedure

- Adaptation strategy allows for the automated generation of off-body grids making it robust to flight plan changes
- Feature-based and adjoint-based indicators can be used to specify the local refinement regions
- Adaptation is performed for a fixed number of cycles or until a convergence criteria is reached

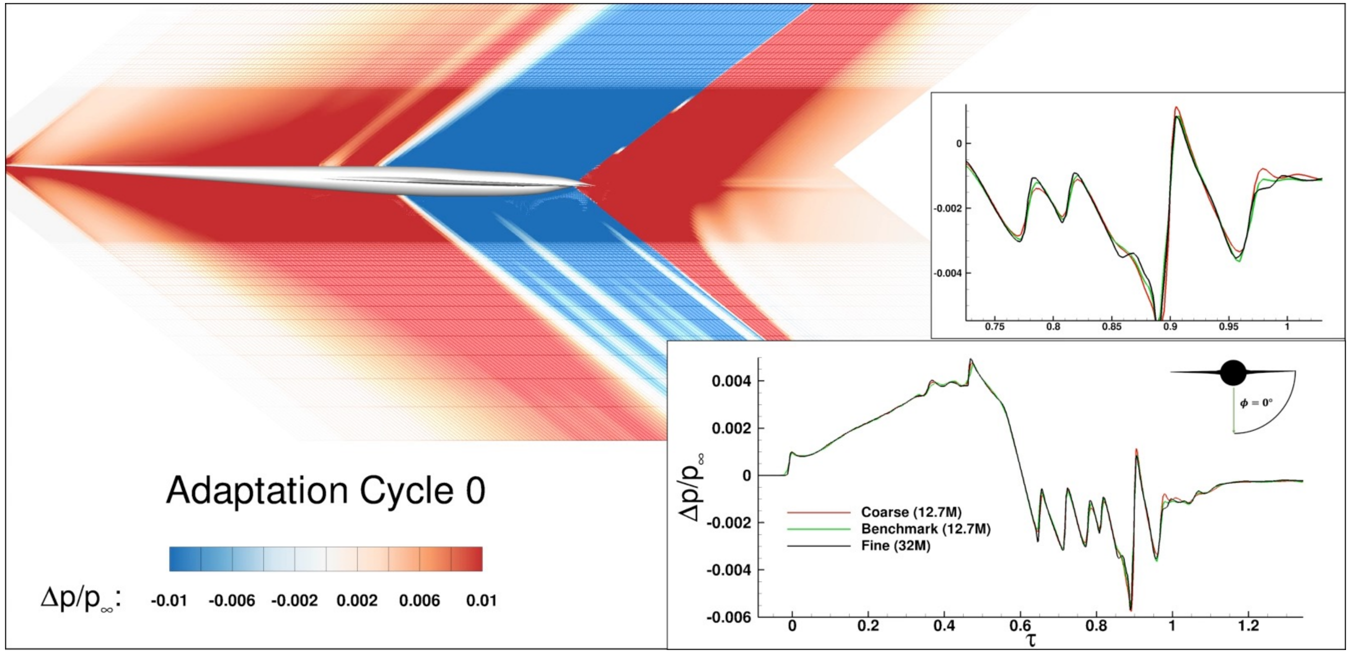

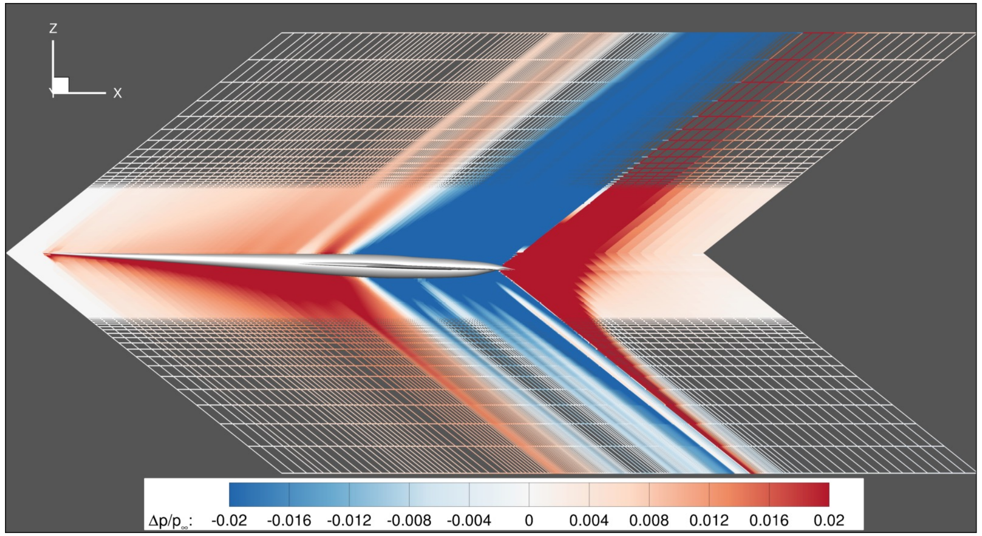

Adjoint Adapted

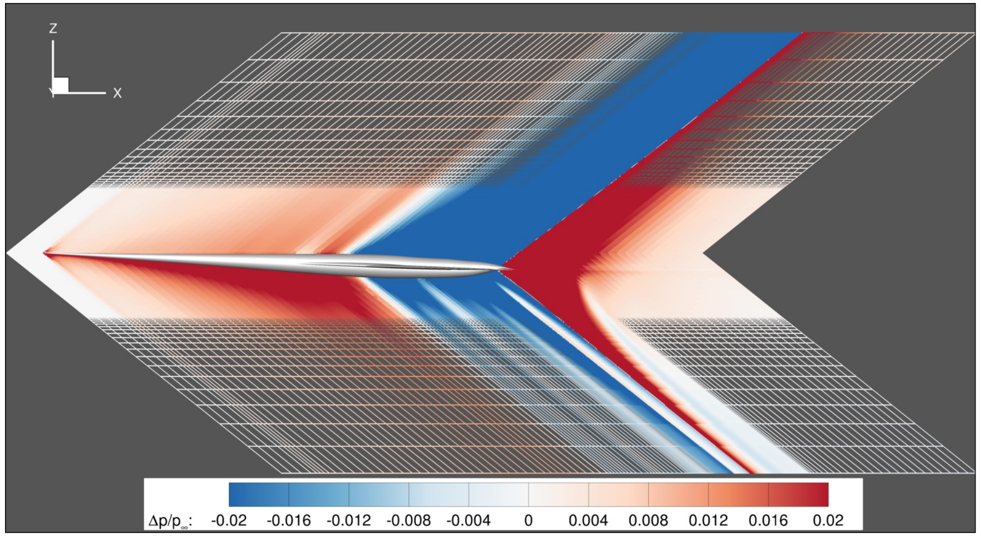

Mach Adapted

Near-field Accuracy Improvement

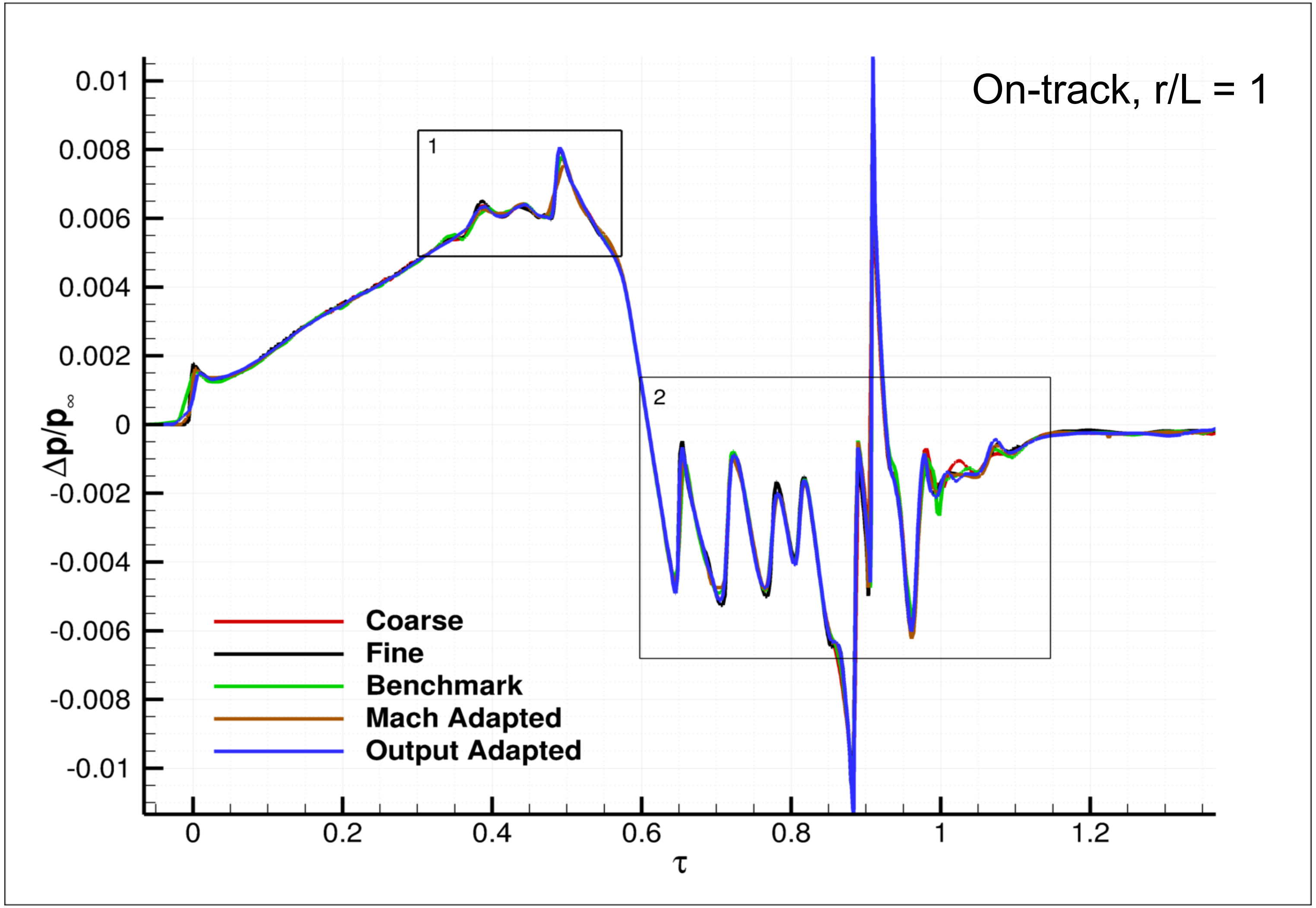

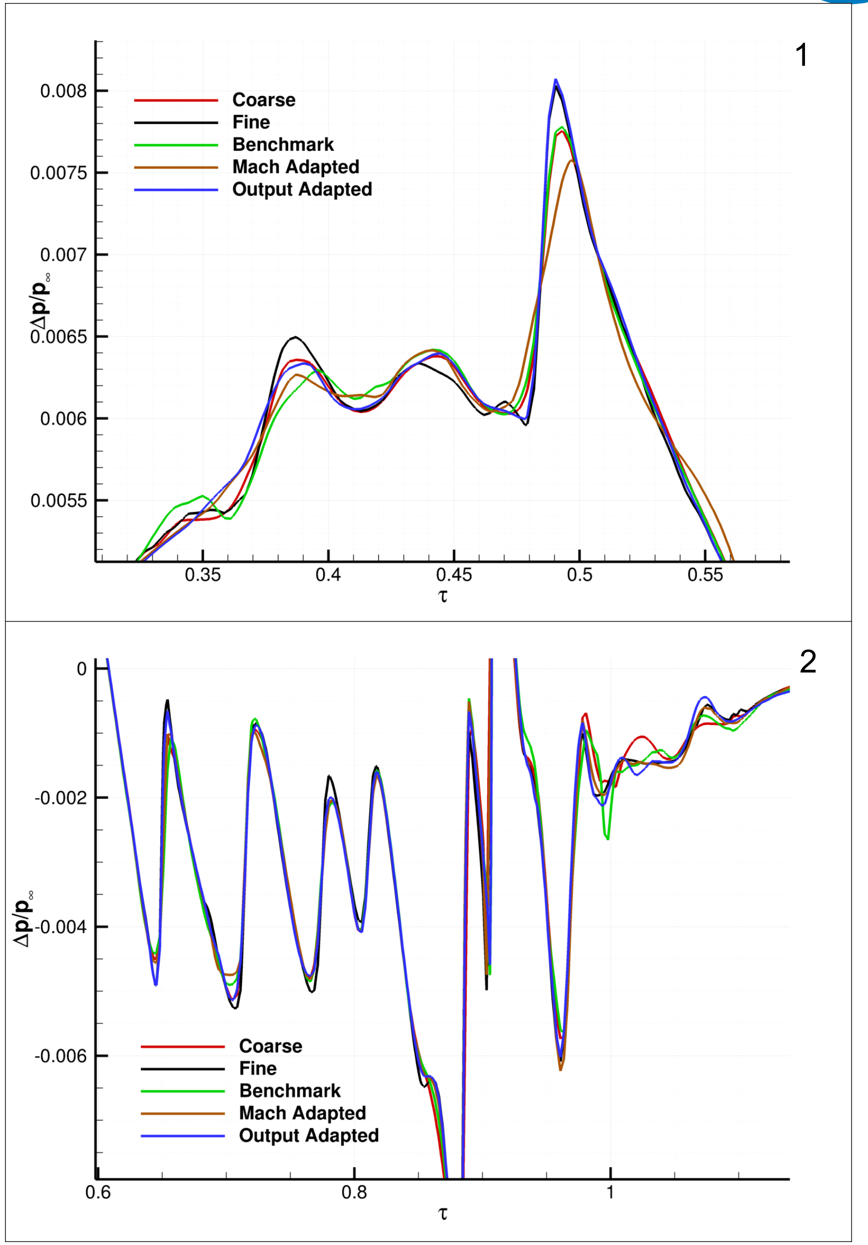

Output-adapted grids typically outperform grids adapted based on Mach-number indicator and the "benchmark" grid-differencing indicator, demonstrated here at 1 body length away

Near-field Accuracy Improvement

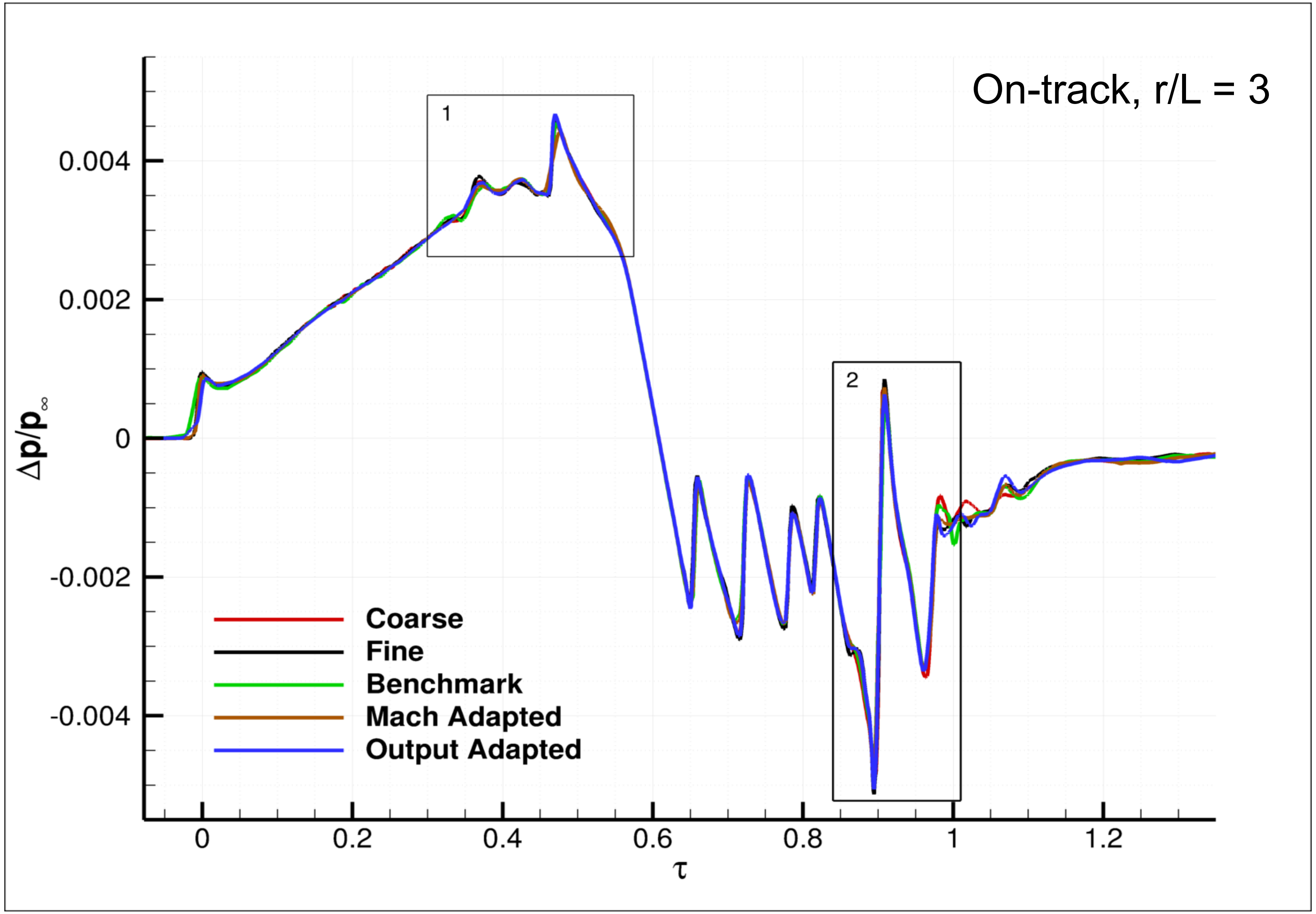

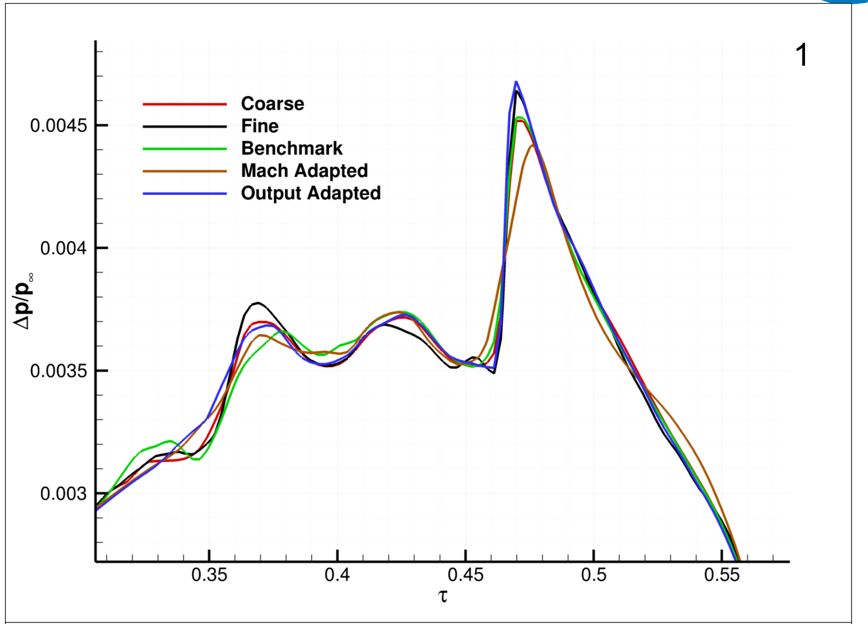

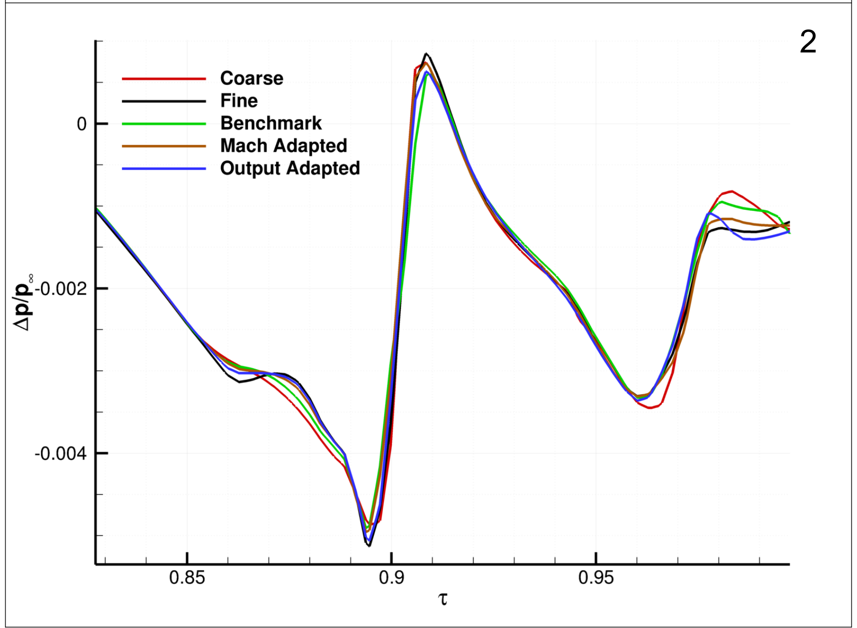

Output-adapted grids typically outperform grids adapted based on Mach-number indicator and the "benchmark" grid-differencing indicator, demonstrated here at 3 body lengths away

Ground Level Accuracy Improvement

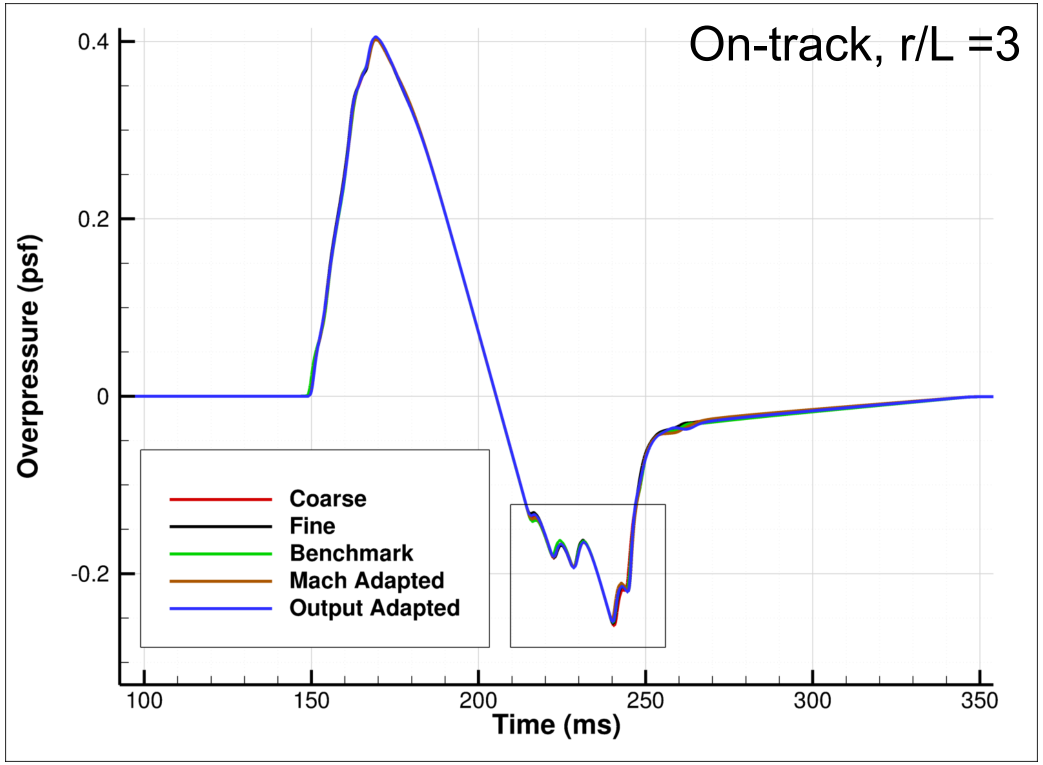

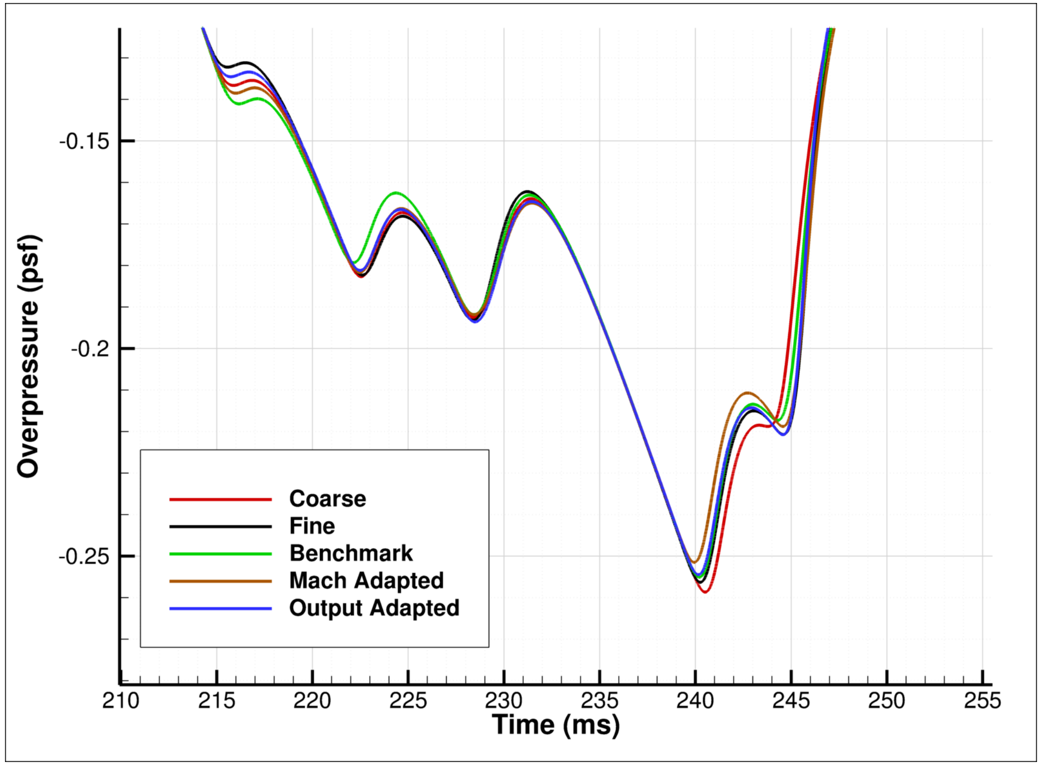

Grid	ASEL [dB(A)]	BSEL [dB]	CSEL [dB(C)]	PL [dB]	ΔASEL	ΔBSEL	ΔCSEL	ΔPL
Fine	62.15	75.96	90.78	75.98	-	-	-	-
Coarse	60.86	75.43	90.71	74.83	2.08e-2	6.98e-3	7.71e-4	1.51e-2
Benchmark	61.50	75.45	90.66	75.18	1.05e-2	6.71e-3	1.32e-3	1.05e-2
Mach Adapted	61.73	75.61	90.66	75.44	6.76e-3	4.61e-3	1.32e-3	7.11e-3
Output Adapted	62.24	75.86	90.74	75.86	**1.45e-3**	**1.32e-3**	**4.41e-4**	**1.58e-3**

Output-adapted grids compare closest to loudness metrics of fine grid solution over other indicators for less cost

Adaptation Cost Savings

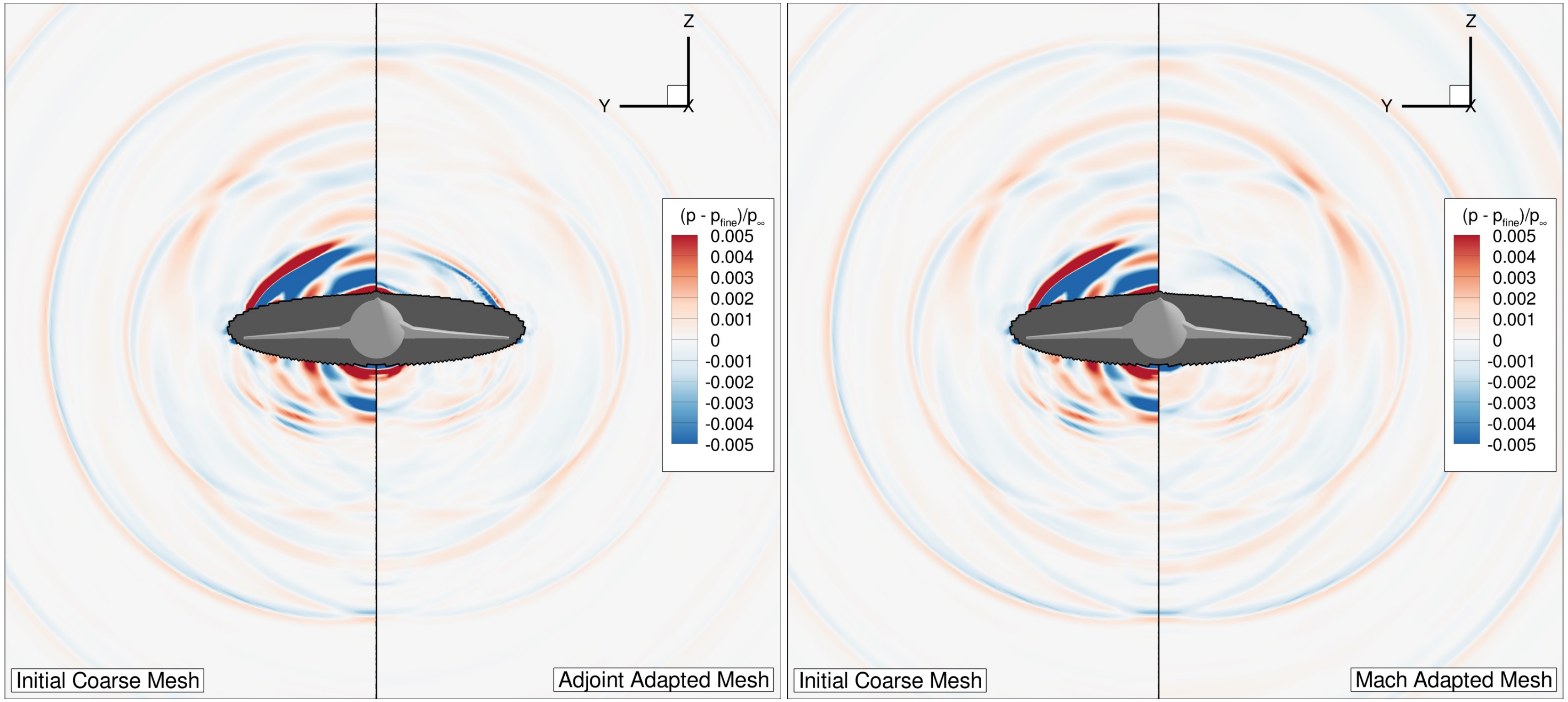

Grid	Connectivity	Primal Solve	Adjoint Solve	Embedding	Adaptation	Restart	**Total**
Coarse	0.14	25.46	-	-	-	-	**25.60**
Benchmark Adapted	0.28	25.46	-	-	0.02	4.70	**30.46**
Mach Adapted	0.29	25.46	-	-	0.01	5.66	**31.42**
Output Adapted	0.28	25.46	0.87	0.17	0.03	5.03	**31.56**
Fine	0.13	55.99	-	-	-	-	**56.12**

Resource usage in CPU-hours for each JWB simulation performed on NASA's Electra supercomputer using 5 Skylake nodes each containing two 20-core Xeon Gold 6148 sockets (2.4 GHz).

LAVA Unstructured Developments

Summary

- Optimized the solver for increased scalability and performance
- Added alternative boundary condition implementations for engine intake:
  - Fixed Mach with varying pressure
  - Fixed average Mach (across the intake) with constant backpressure that is iteratively adjusted to achieve the target value
- Improved far-field boundary condition implementation with a characteristic-based, non-reflecting method
- Improved quality and speed of line/surface data probing capability used to extract the pressure signal
- Implemented features to interface with the Space Marching solver
- Improved automation and speed of our meshing practices
- Expanded solver testing
- Performed code-to-code verification with LAVA Curvilinear for X-59 and sonic boom workshop cases

Significance

- LAVA Unstructured is being used with confidence to populate boom solution databases efficiently and perform in-house code-to-code comparisons

LAVA Curvilinear Grid Generation: Hole-cutting

- Overset grids may be present inside geometry and must be blanked to be excluded from computational domain. Hole-cutting blanks grid nodes within a defined cutting geometry
- OVERFLOW hole-cutting can be as time-intensive as grid scripting since building its hole cuts is both manual and iterative
- LAVA hole-cutting implicitly determines geometry surface and blanks grid nodes within it, and removes geometric ambiguity with simple hole cuts
- For the C608:
  - **OVERFLOW hole-cutting method**: 33 manually generated hole-cuts, 231 cutting instructions, **7 minutes** wall time
  - **LAVA hole-cutting method**: 5 hole-cuts (simple shapes)**, 36 seconds** wall time

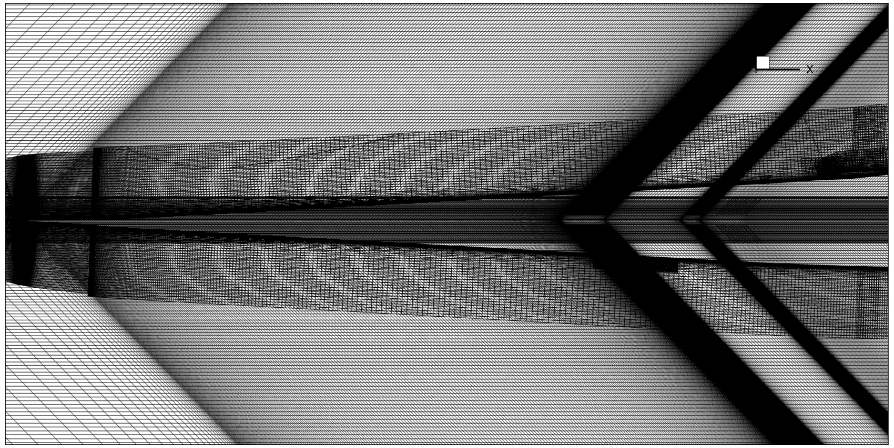

Top: X-59 nose before hole-cutting and overlap
Bottom: after

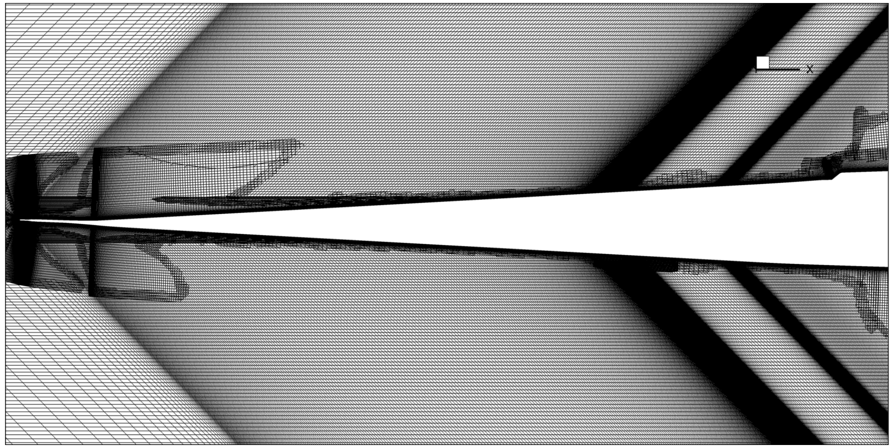

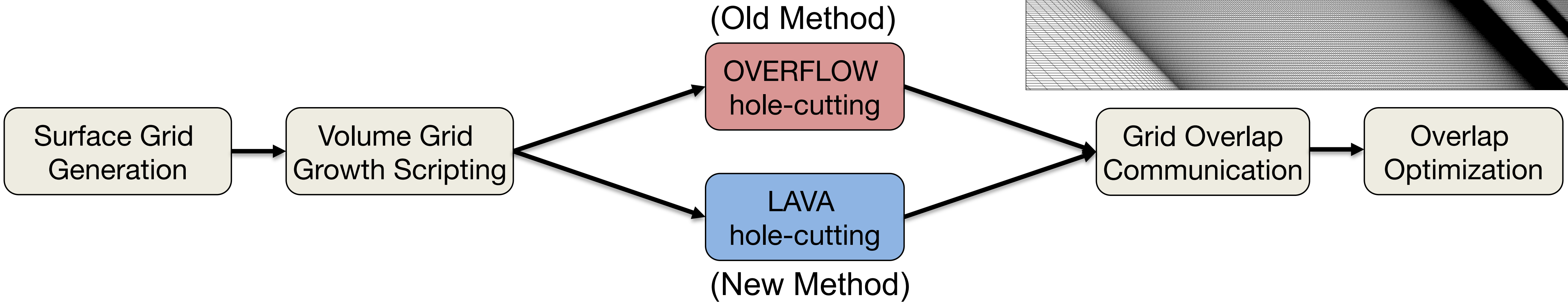

Glenn Wind Tunnel Comparisons with LAVA

- 1.62% Scale model of C612A configuration of X-59
- Tested in Glenn 8x6 wind tunnel in 2021
- Four NASA codes compared

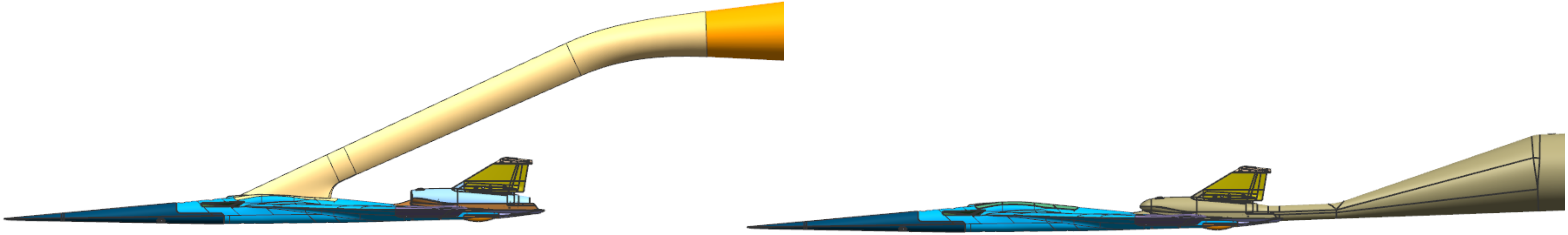

Left: wind tunnel model, blade mount; Right: sting mount

*NASA/TM–20220011496

Glenn Wind Tunnel Comparisons with LAVA

- Wind tunnel database consisted of 40 cases in LAVA Unstructured and LAVA Curvilinear including changes in:
  - Mach number
  - Angle of attack and roll angle
  - Mount choice (blade strut vs sting)
  - Control surface deflections (flaps, tail, etc)
- Curvilinear grids were built to interface with and utilize the space marching solver; Unstructured grids did not use space marching
- Unstructured mesh: 142M cells
- Curvilinear RANS (near field) mesh: 80M nodes
- Each individual case is meshed and solved in under 8 hours excluding queue time

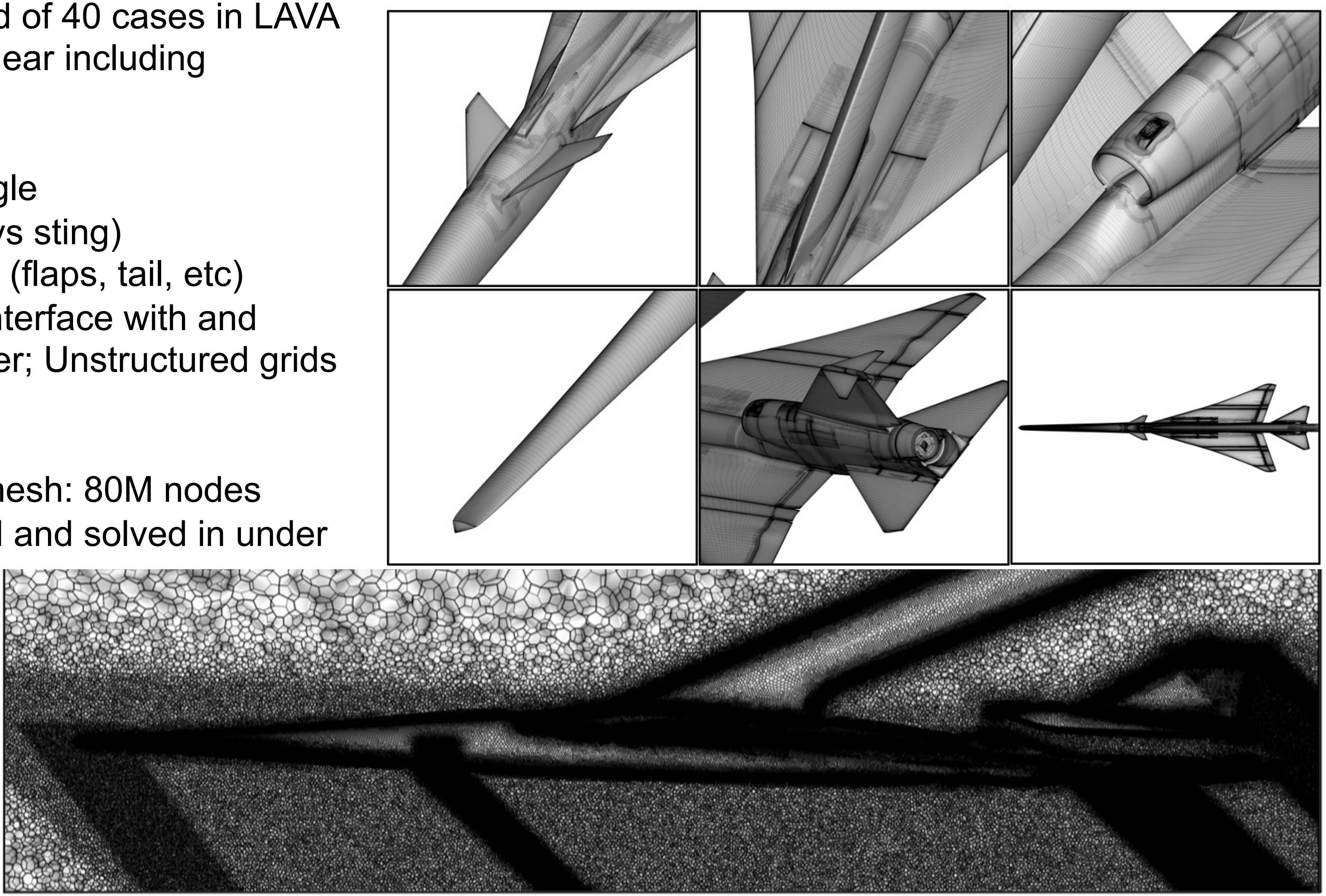

*NASA/TM–20220011496

Top: Curvilinear surface mesh of wind tunnel model; Bottom: Unstructured volume grid

Glenn Wind Tunnel Comparisons with LAVA

- LAVA solutions compare favorably to experiment and other solvers for all cases
- Largest differences between experimental and code-to-code in:
  - Inlet shock ($x \approx 14$in)
  - Ttail waves ($x \approx 21$in)

- Some difference expected from wind tunnel spatial averaging:

  "To get better-quality data than just from single pressure signature measurements on the rail, a linear actuator was used to measure signatures at different longitudinal positions (typically 26) on the rail. These X sweeps of the model enabled spatial averaging of the signatures from the different positions, which greatly reduced the scatter of the data, and […] ***did result in some rounding of the peaks*** *in the signatures."* - NASA/TM–20220011496

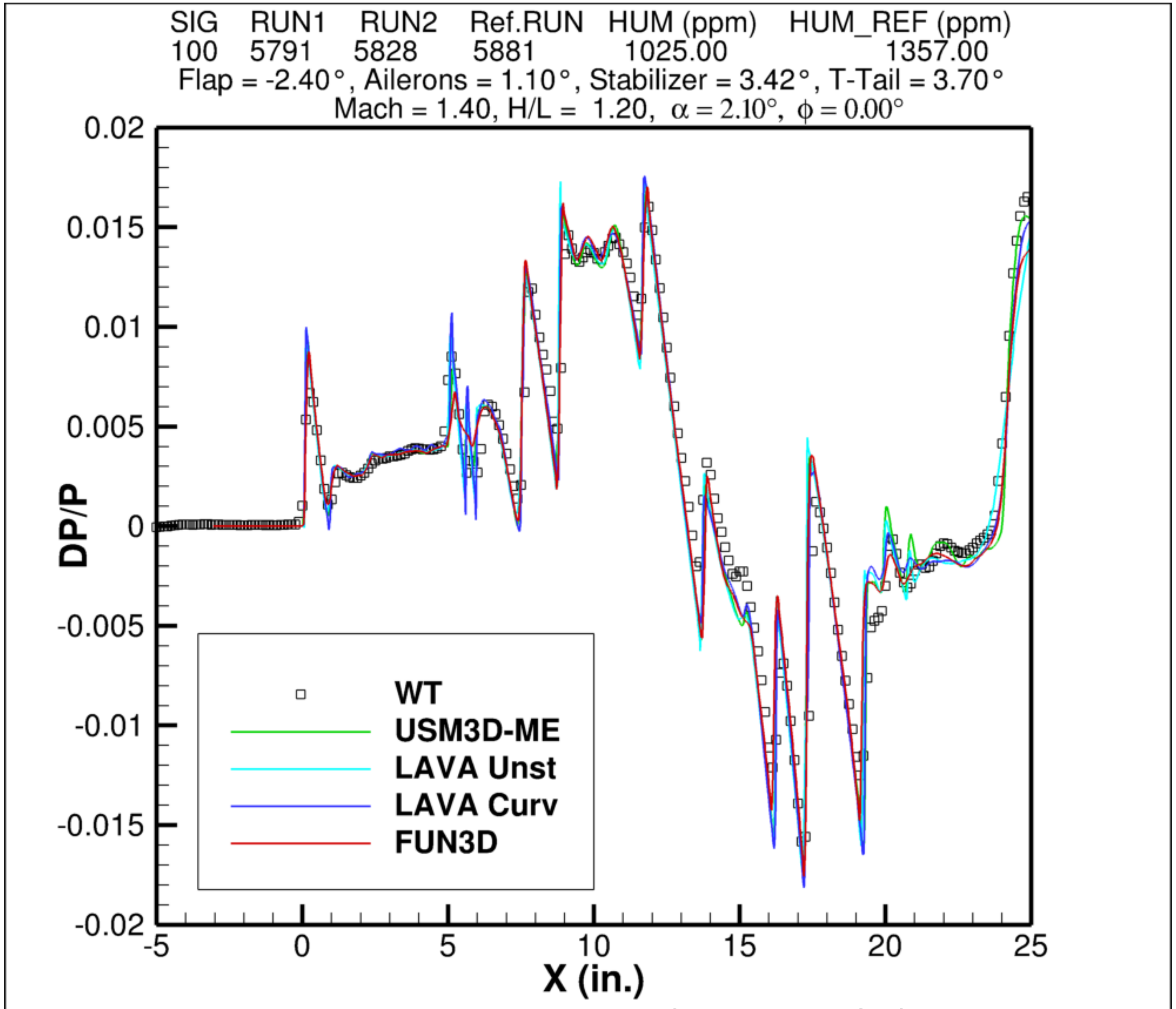

Blade mount, baseline deflections -NASA/TM–20220011496

Glenn Wind Tunnel Comparisons with LAVA

Sting mount, baseline deflections

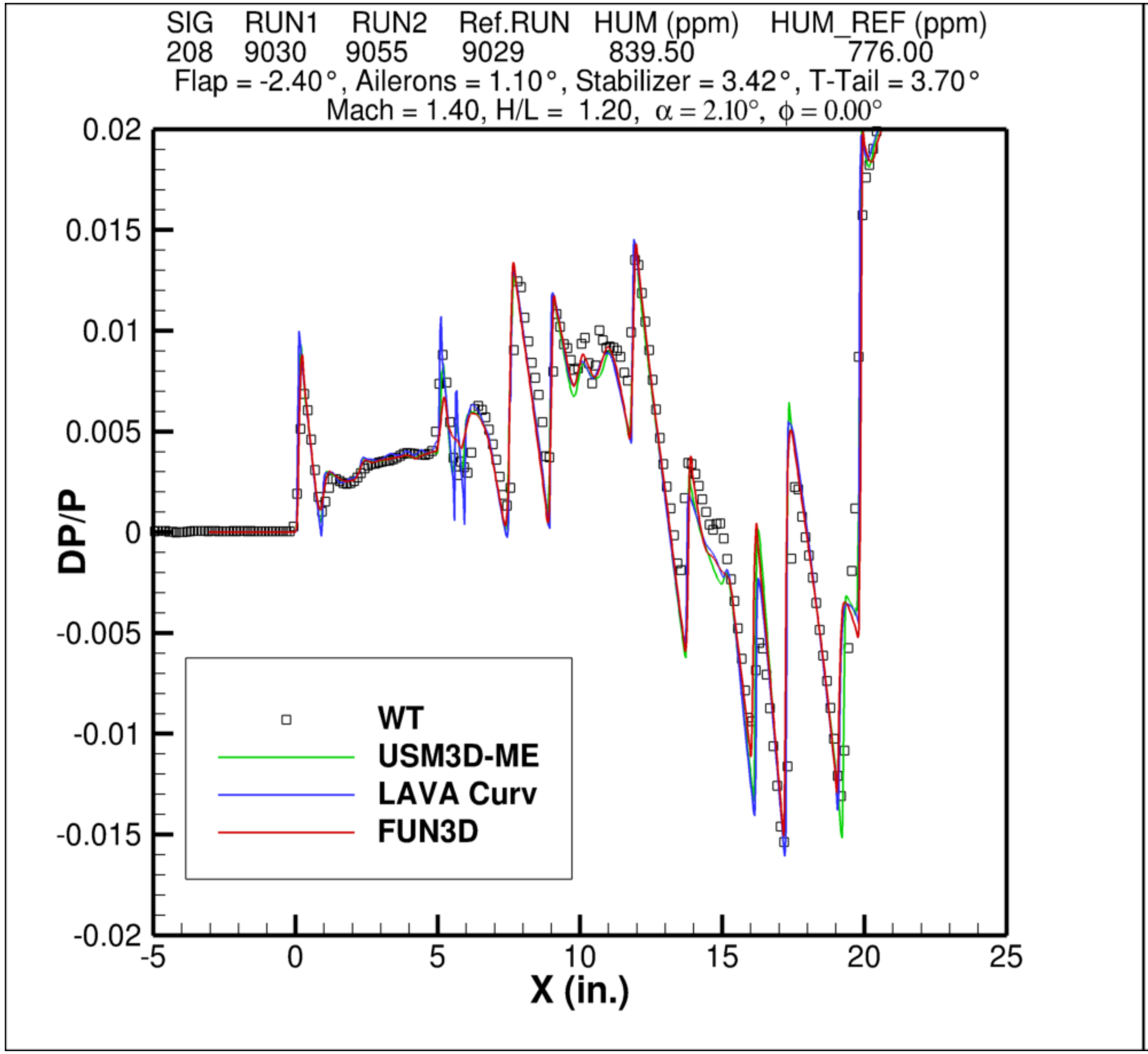

Blade mount, α deflection

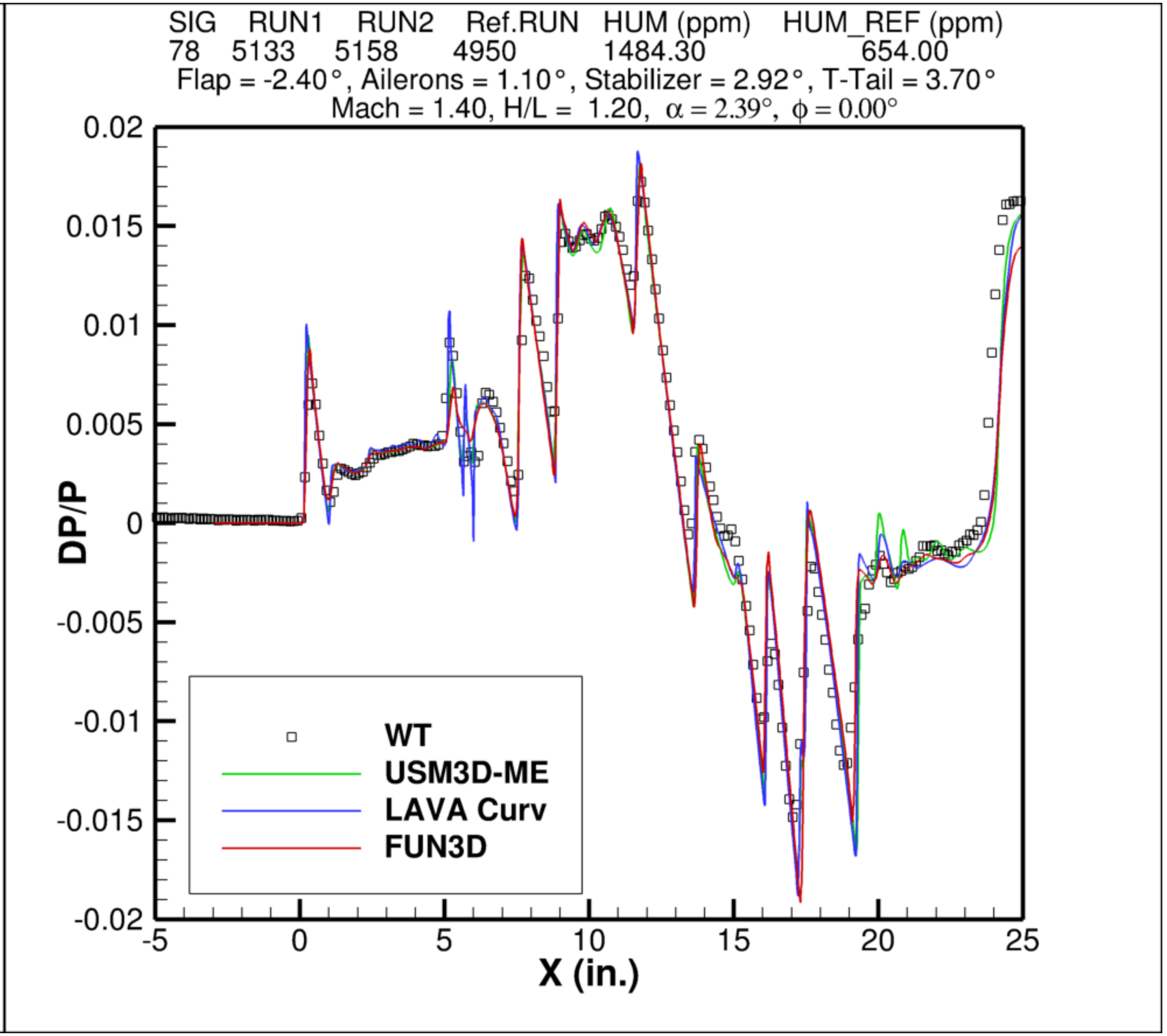

*NASA/TM–20220011496

Glenn Wind Tunnel Comparisons with LAVA

- Applied adjoint-based off-body mesh redistribution capability
- Developed refined curvilinear mesh (225M points compared to 80M) for comparison
- Adjoint-adapted solution (85M points) compares favorably to fine grid solution with significantly fewer grid points
- Redistribution is constrained by grid size, which resulted in decreased local resolution upstream and increased resolution downstream

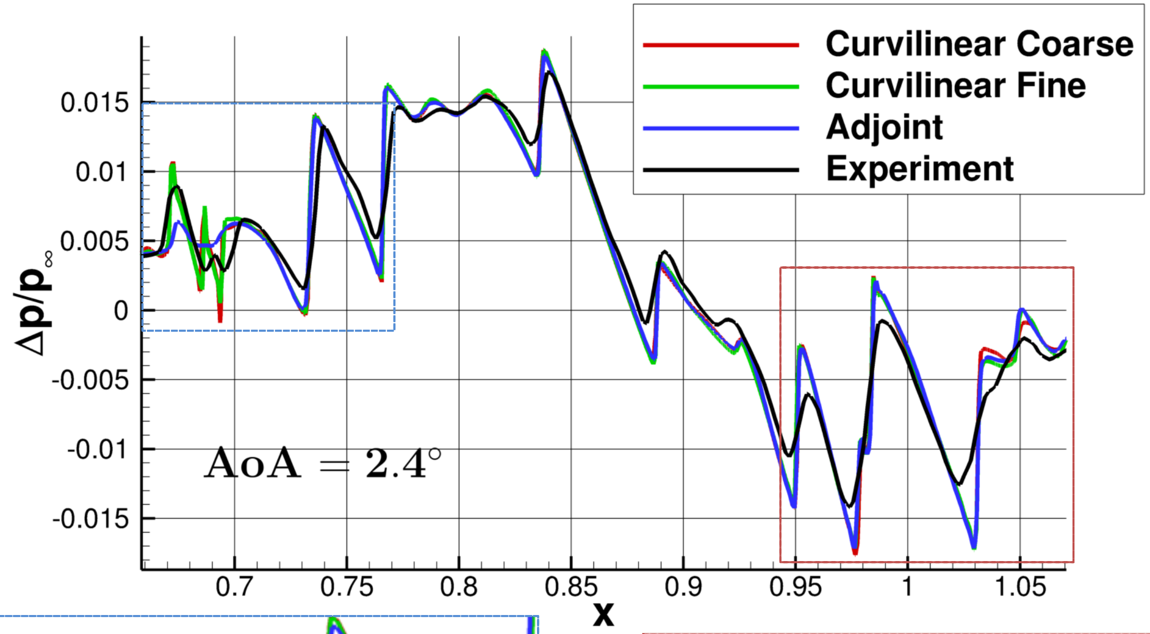

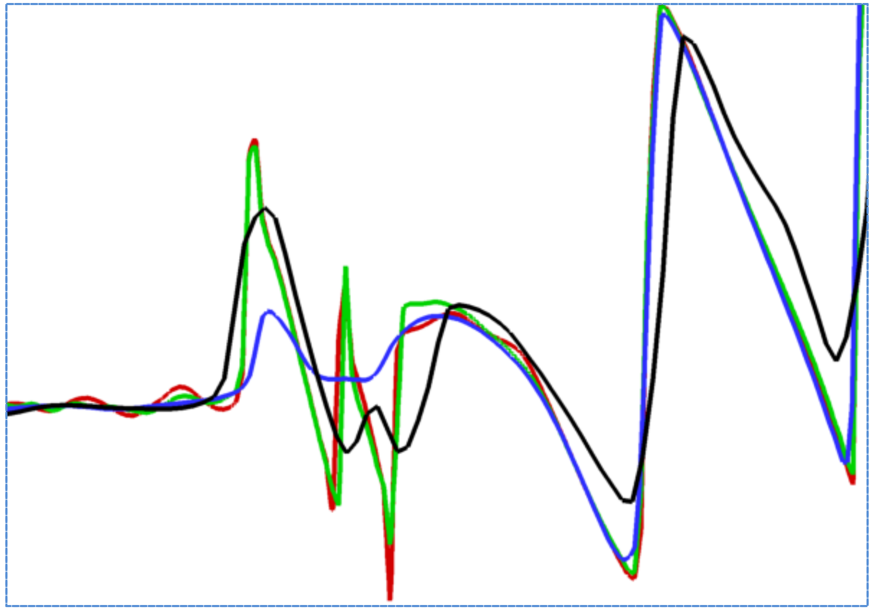

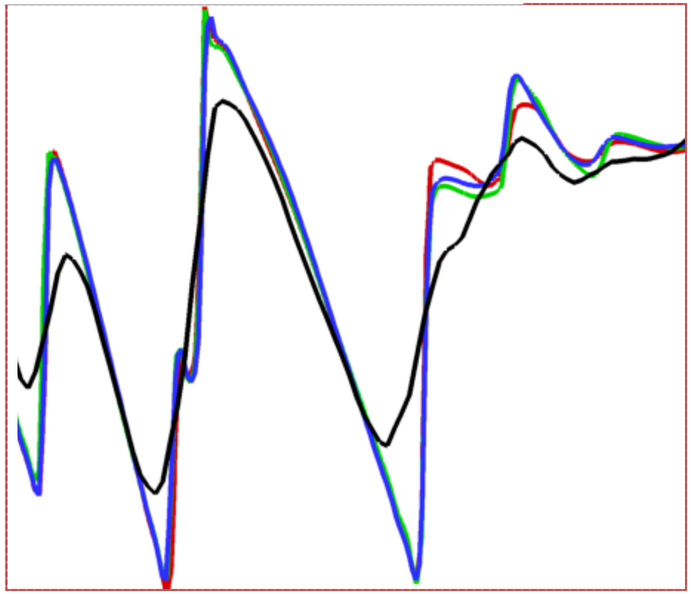

Left: upstream (low grid resolution)
Right: downstream (high grid resolution)

X-59 C608 Aircraft

Reference length : $L_{ref} = 27.432\ m$

Cruise Altitude : 16,215 m

Mach = 1.4, Re/m = 4.3 million, and $\alpha = 2.15^{\circ}$

Front View

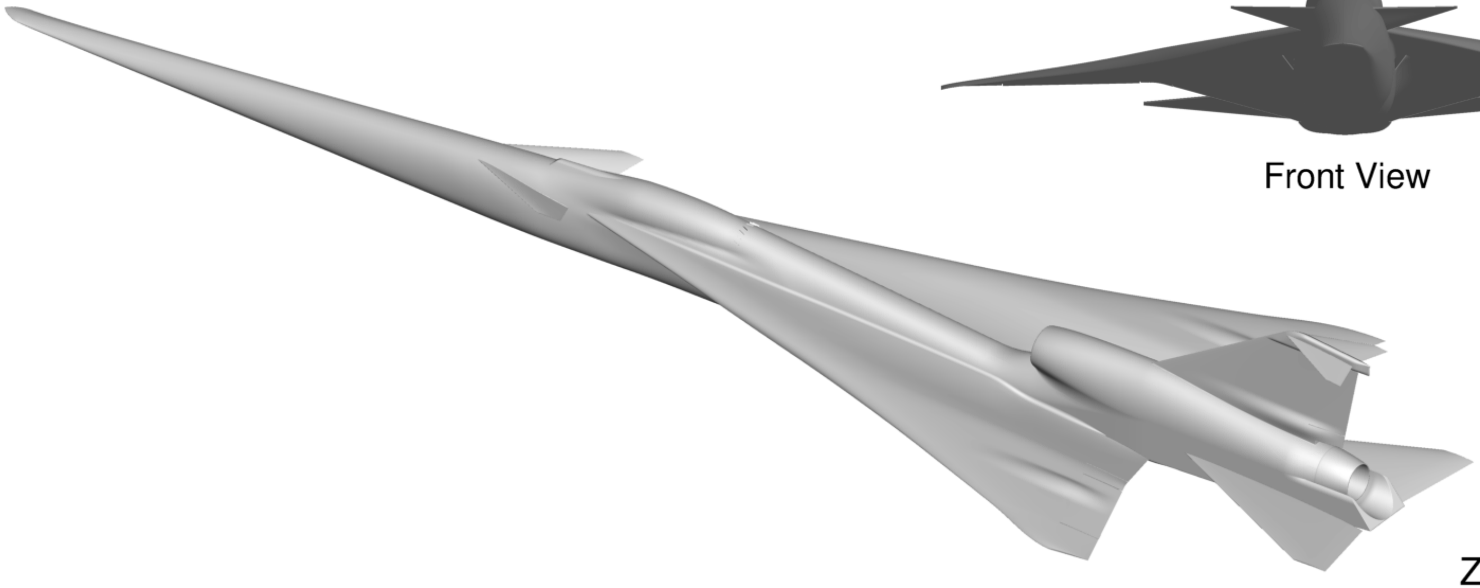

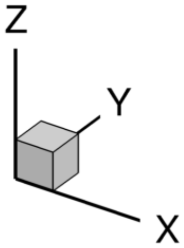

Side View

C608 Coarse Grid Adaptation

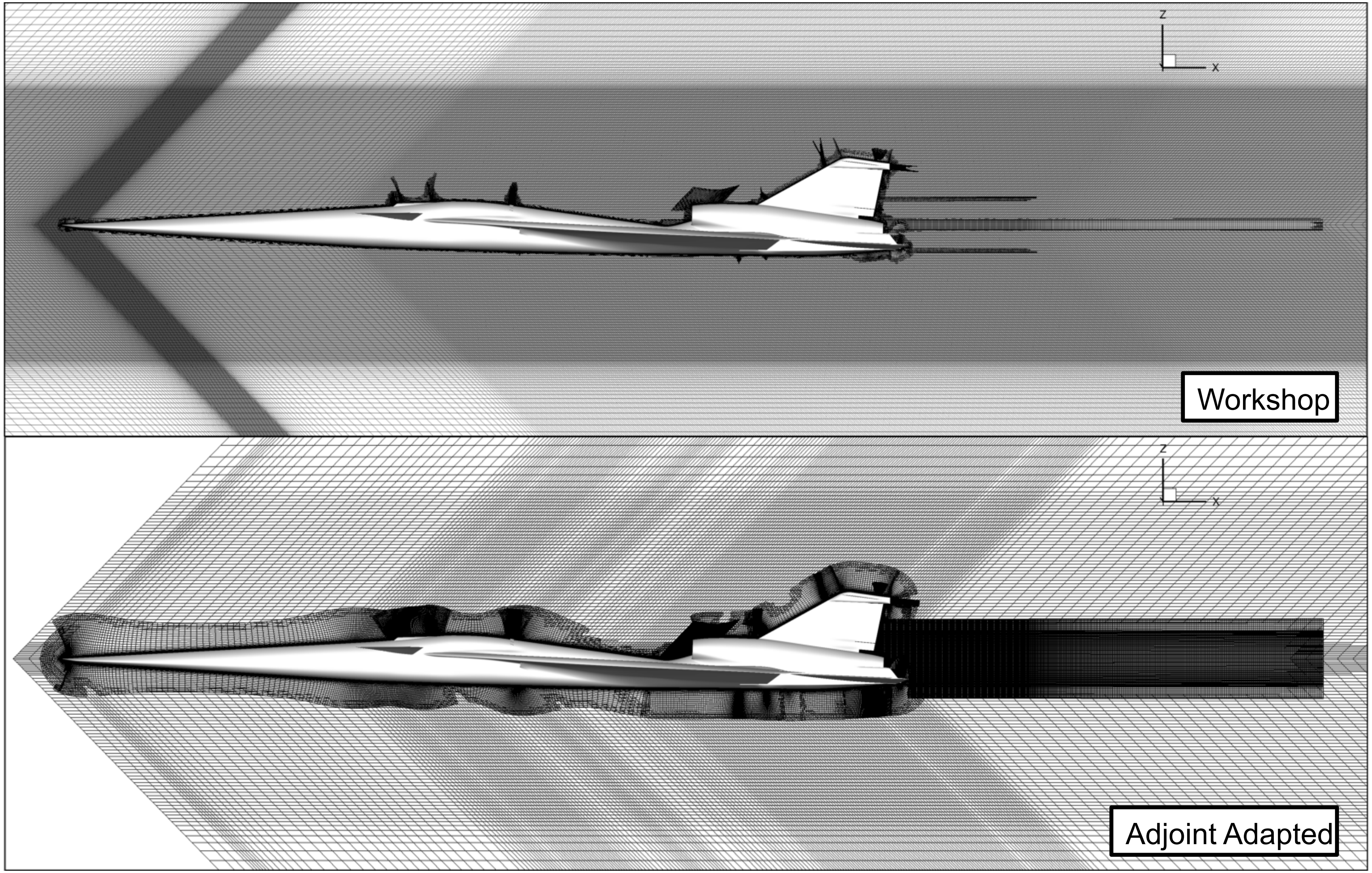

Grids redistributed based on adjoint indicator automatically determine refinement regions

C608 Coarse Grid Adaptation

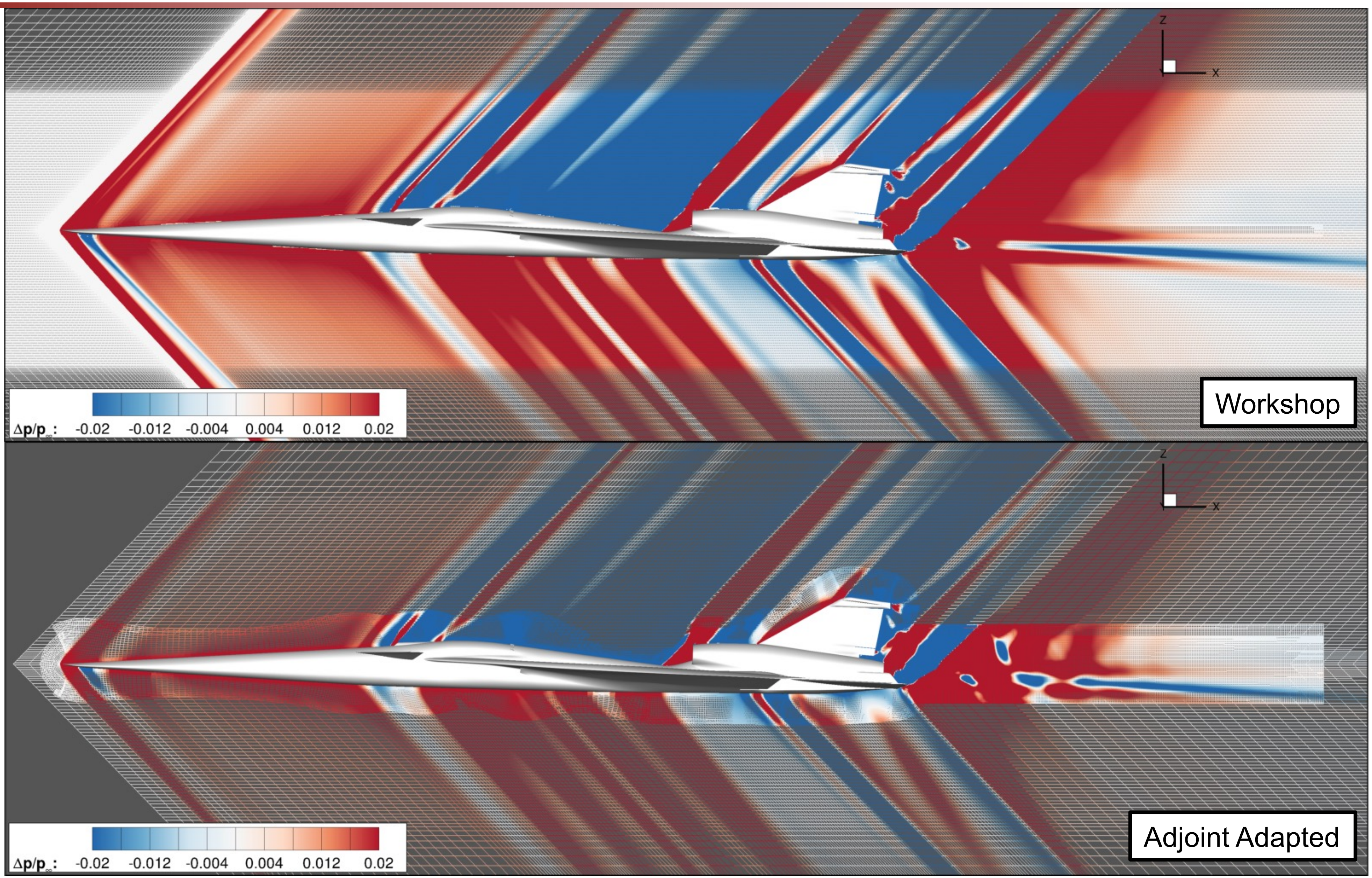

Solutions on adjoint-adapted grids compare favorably with manually generated grids

C608 Medium Grid Pressure Signatures

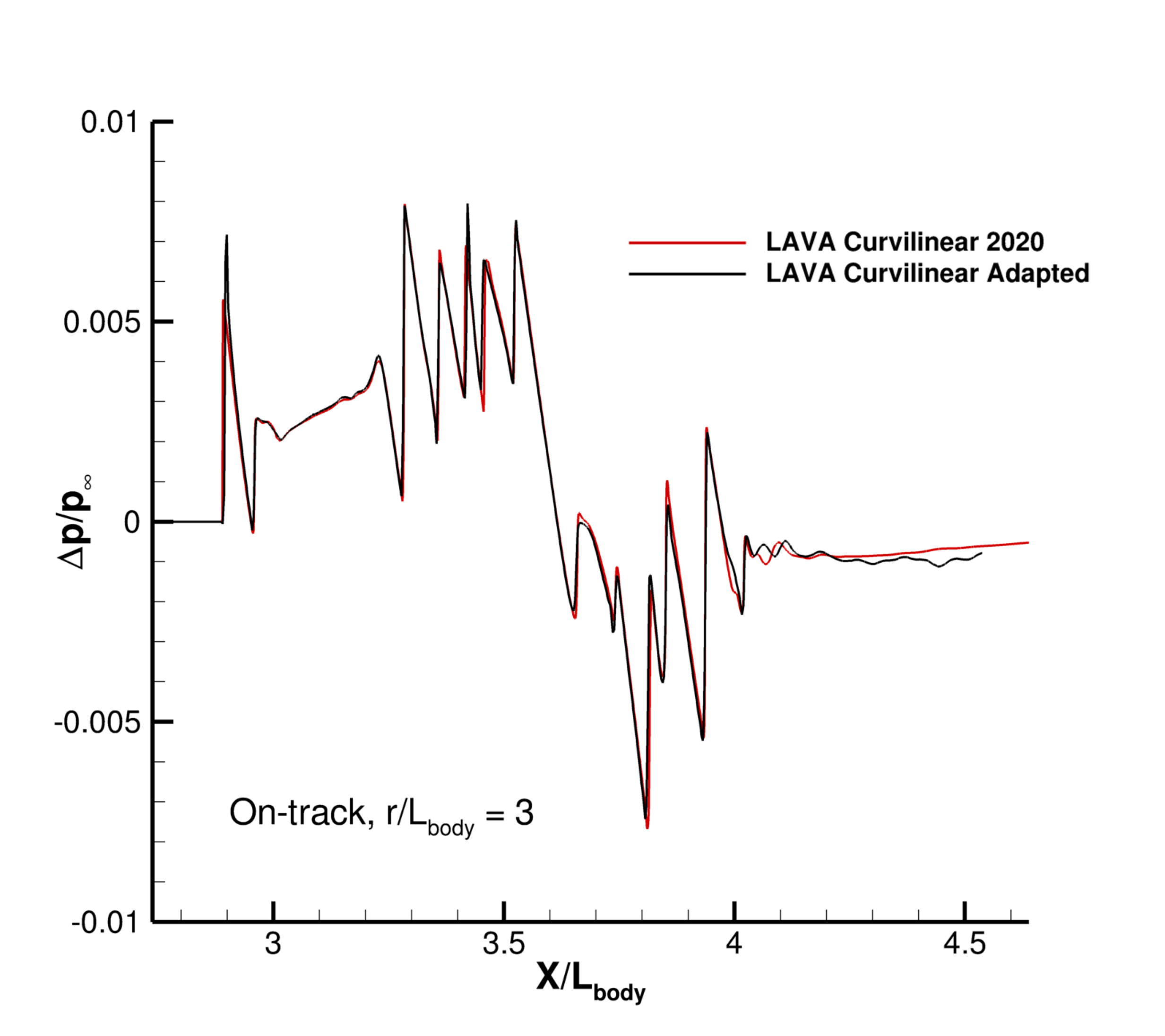

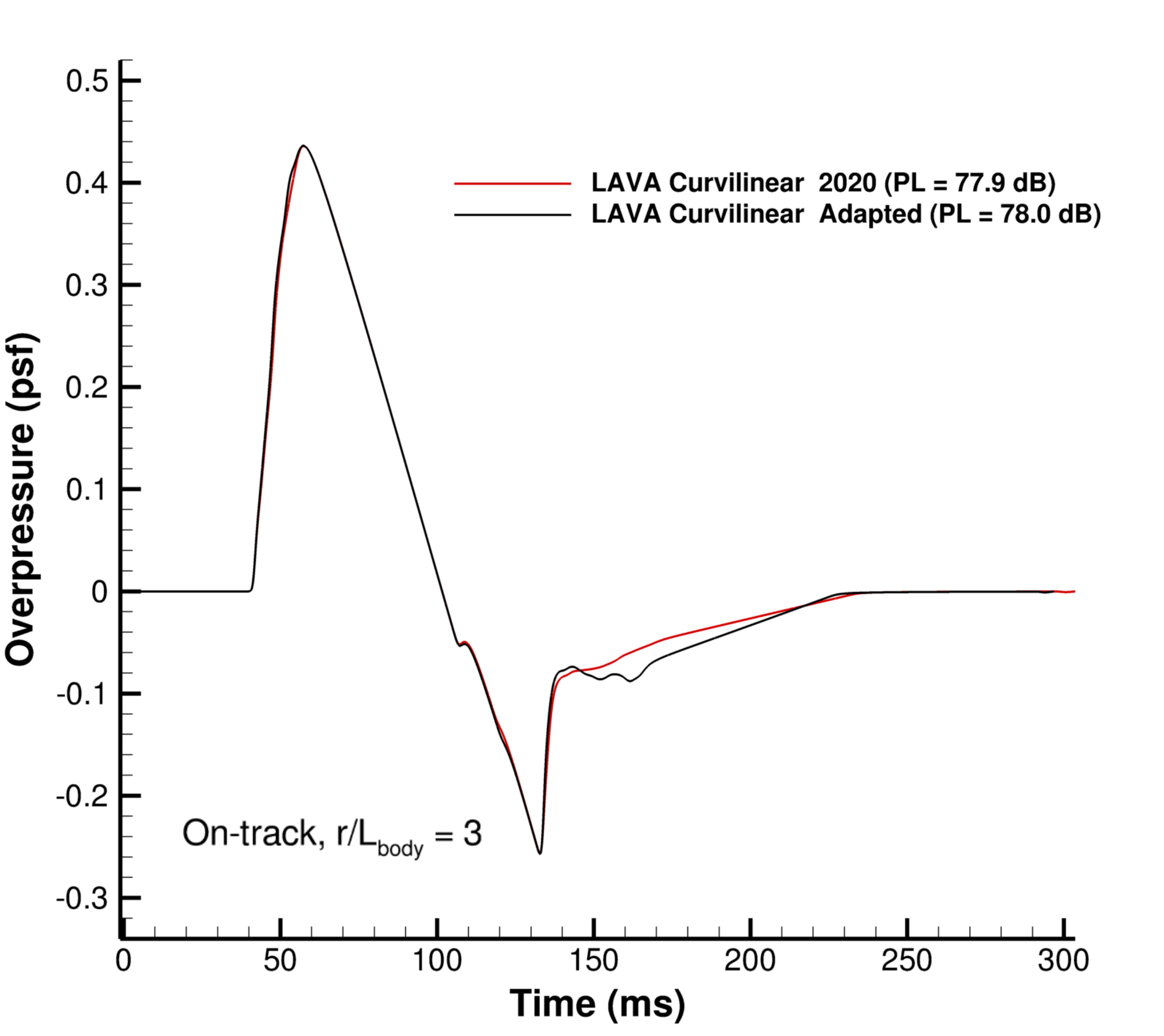

Loudness predictions on adjoint-adapted grids are consistent with manually generated grids

C608 Demonstration

- Automated off-body and manual grid generation procedures are compared using fixed medium level near-body grids from the 3rd AIAA Sonic Boom Prediction Workshop

- Overset connectivity is computed using LAVA's hole cutting algorithm

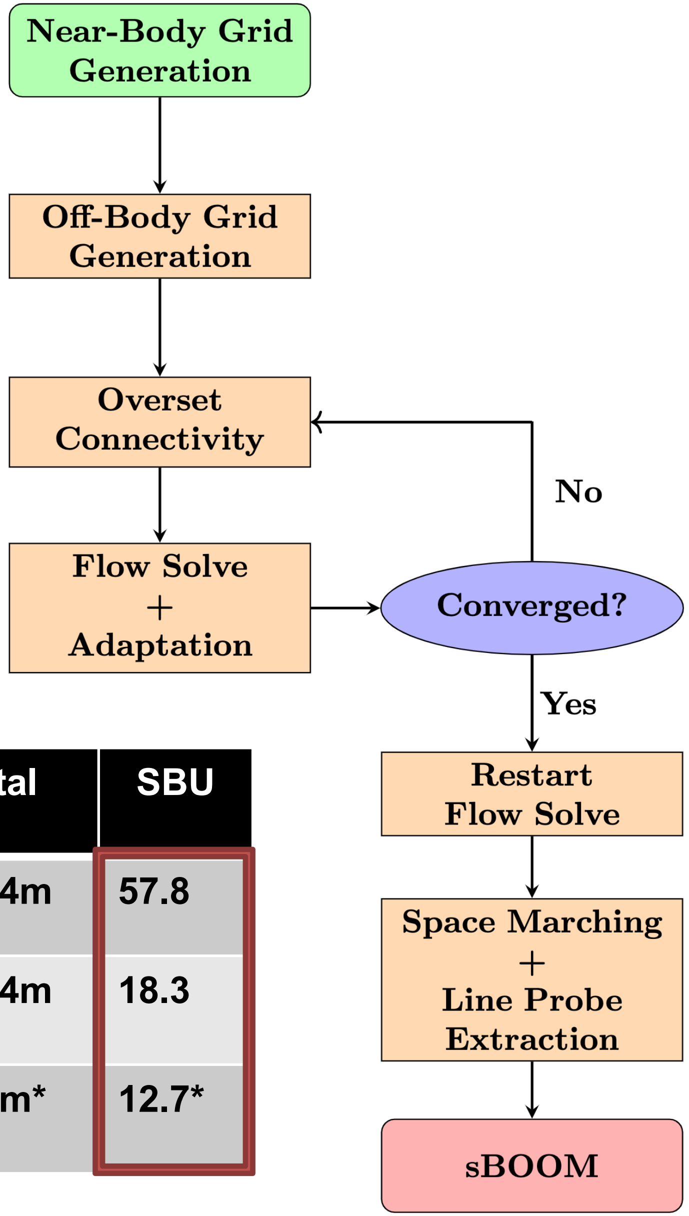

	Total Nodes (In Millions)	Degrees of Freedom (In Millions)	Nodes per Core	Nodes per Core (Re-factored)
Medium (2019)	161.990	127.379	126,931	318,475
Medium Adapted	75.271	53.412	-	317,929

	Connectivity	Primal Solve	Dual Solve	Embedding	Adaptation	Restart	Total	SBU
Medium (2019)	2hr 24m		-	-	-	-	**2hr 24m**	**57.8**
Medium (Re-factored)	1hr 24m		-	-	-	-	**1hr 24m**	**18.3**
Medium Adapted	1m*	1hr 15m	6m 35s	2m 5s	1m 35s	44m 9s	**2hr 7m***	**12.7***

* Estimated times based on coarse grid study.

X-59 Flight Model

- X-59 Flight Model
  - Reference length : $L_{ref} = 27.432\ m$
  - Cruise Altitude : 16,215 m
  - Mach = 1.4, Re/m = 4.6 million, and $\alpha = 2.09^{\circ}$

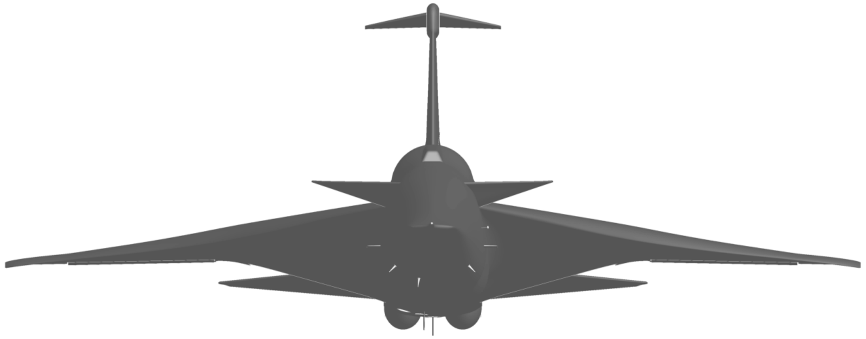

Front View

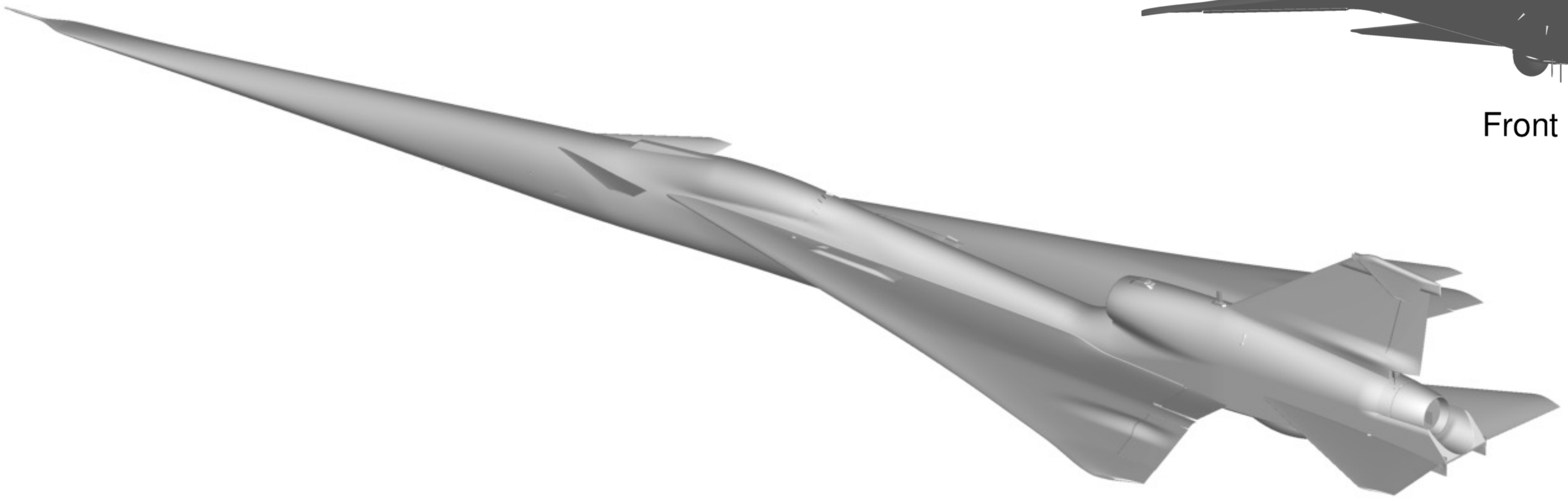

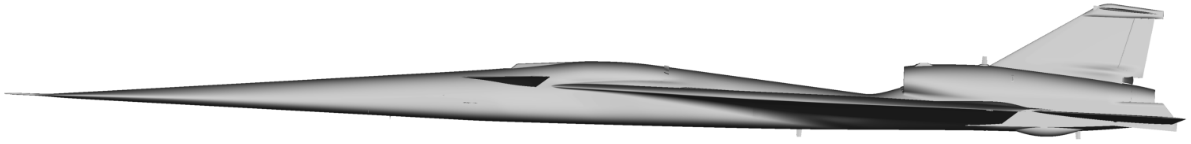

Side View

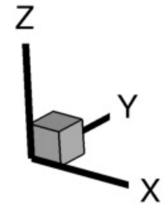

Off-Body Comparisons: Adjoint Adapted vs. Expert User

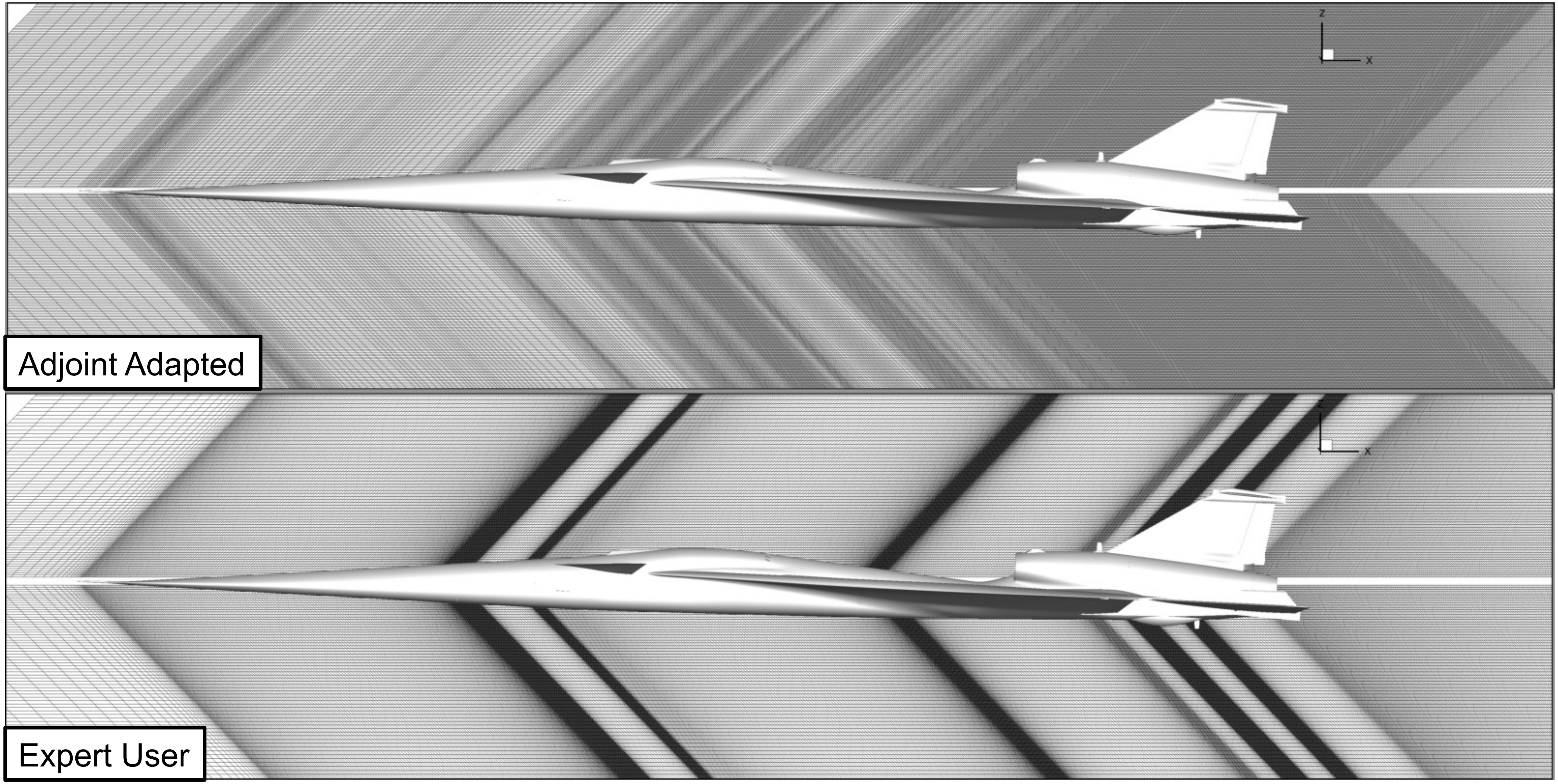

Adjoint adapted grids automatically determine important refinement regions based on output indicator

Adjoint Adapted vs. Expert User

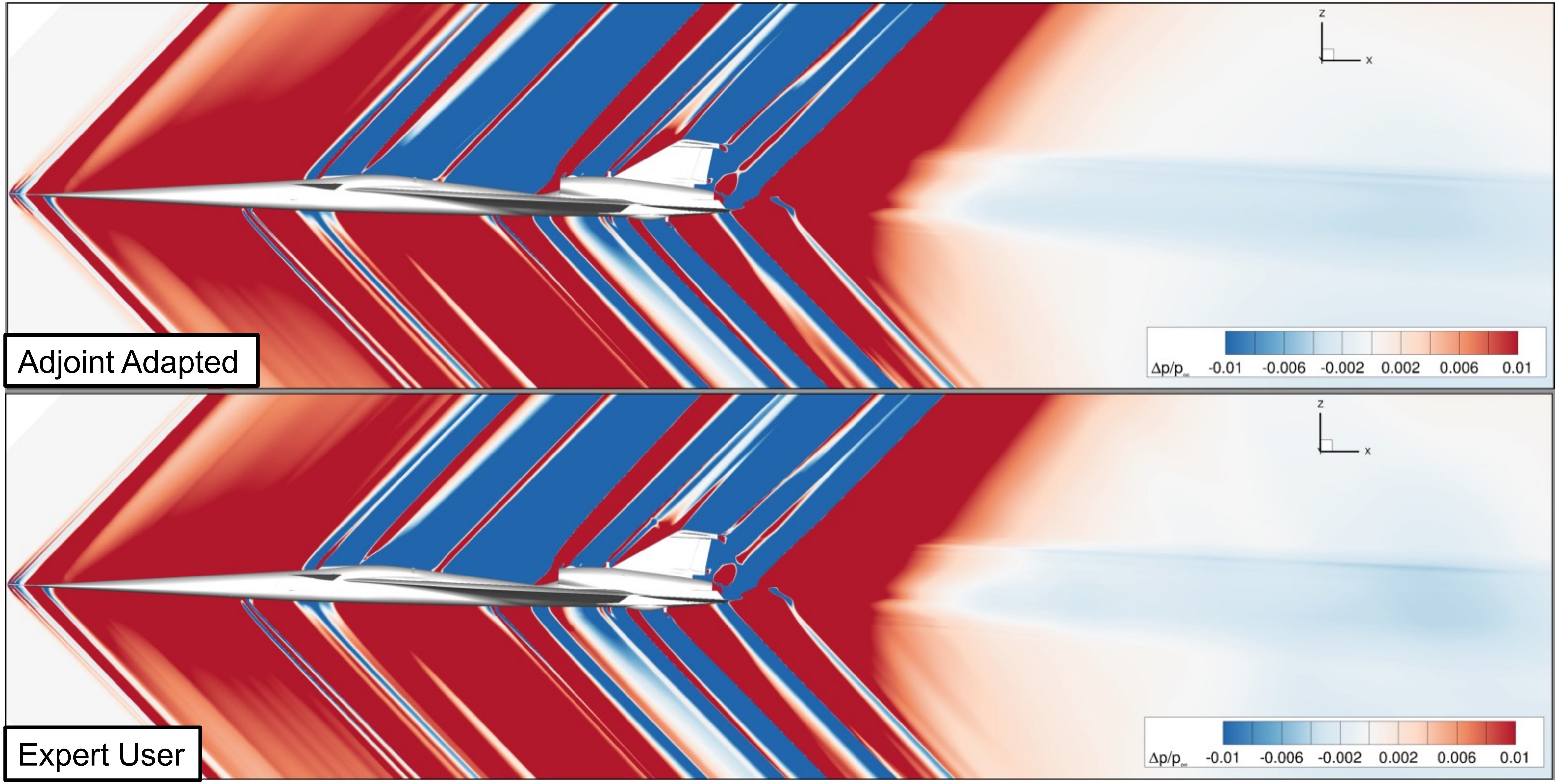

Flow solution (pressure disturbance) on adjoint adapted and manually generated grids appear qualitatively consistent

Near-Field Propagation Difference via Space Marching

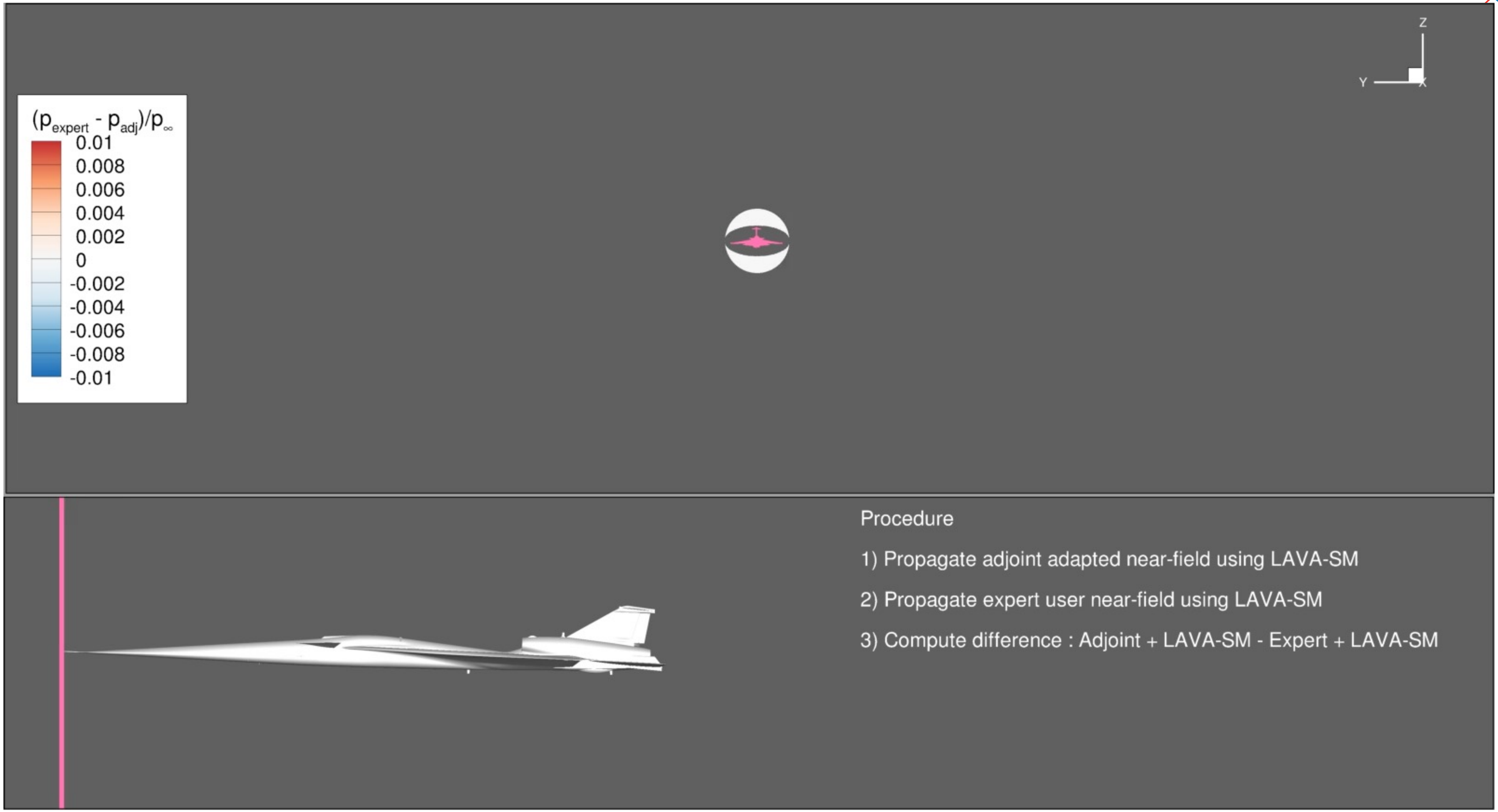

Space marching enables tracing solution differences between grids back to the vehicle to determine sources of solution difference

Adjoint Grid Adaptation: Near-Field Signatures

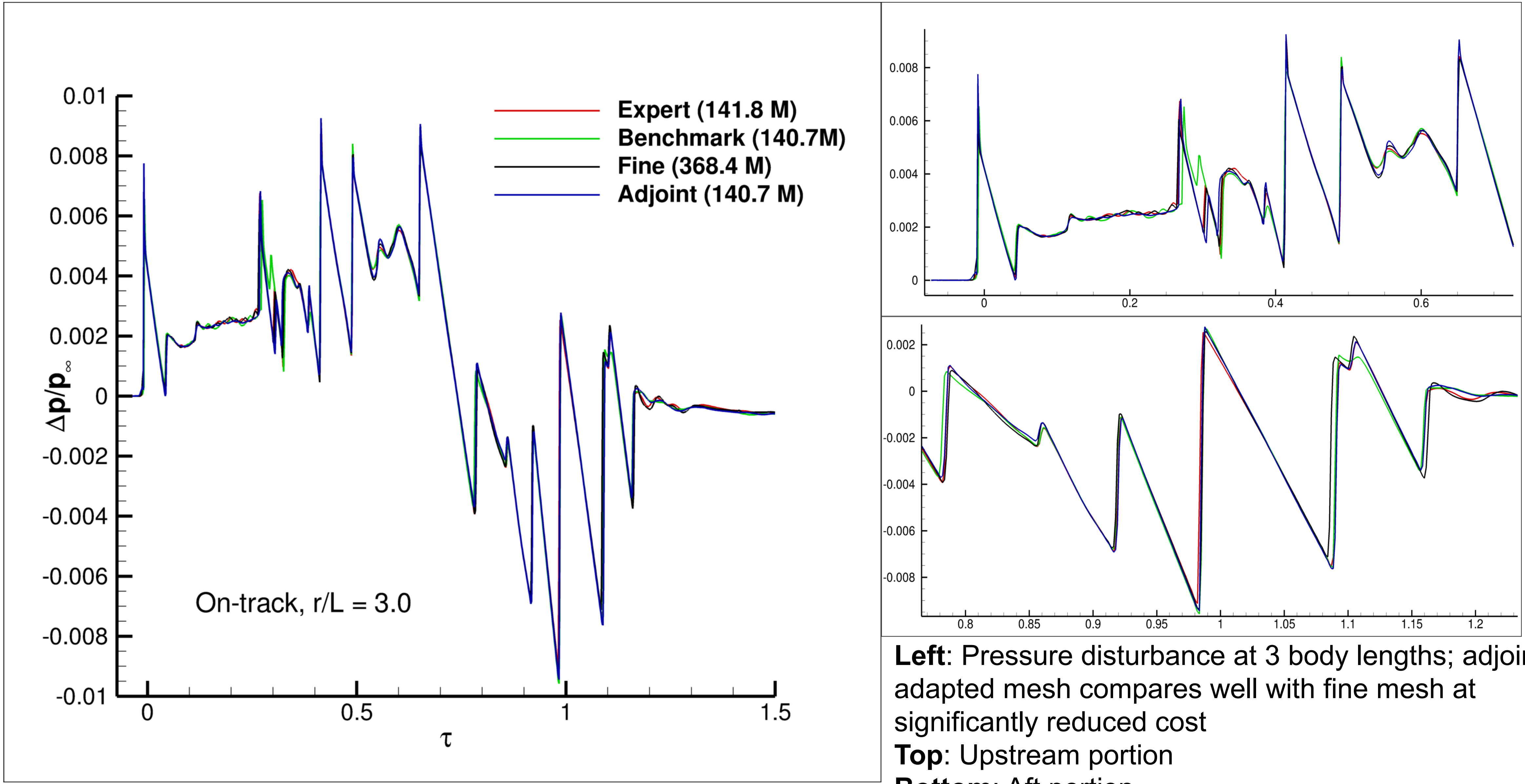

Left: Pressure disturbance at 3 body lengths; adjoint-adapted mesh compares well with fine mesh at significantly reduced cost

Top: Upstream portion

Bottom: Aft portion

Adjoint Grid Adaptation: Ground-Level Signatures

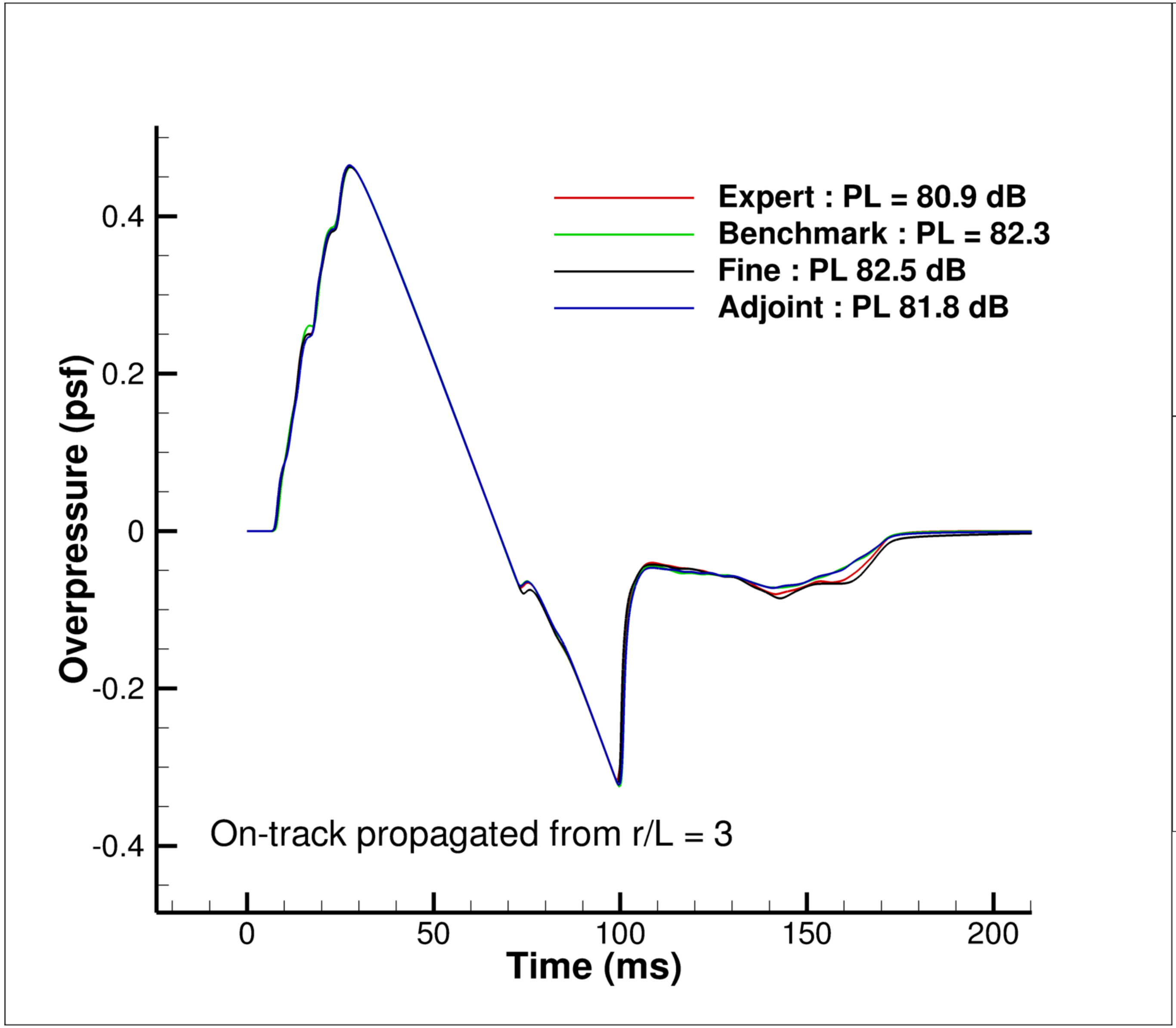

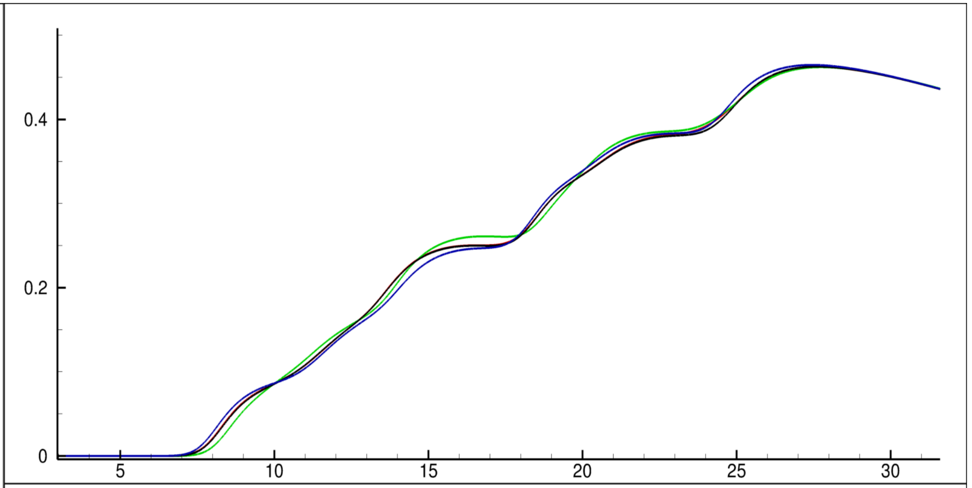

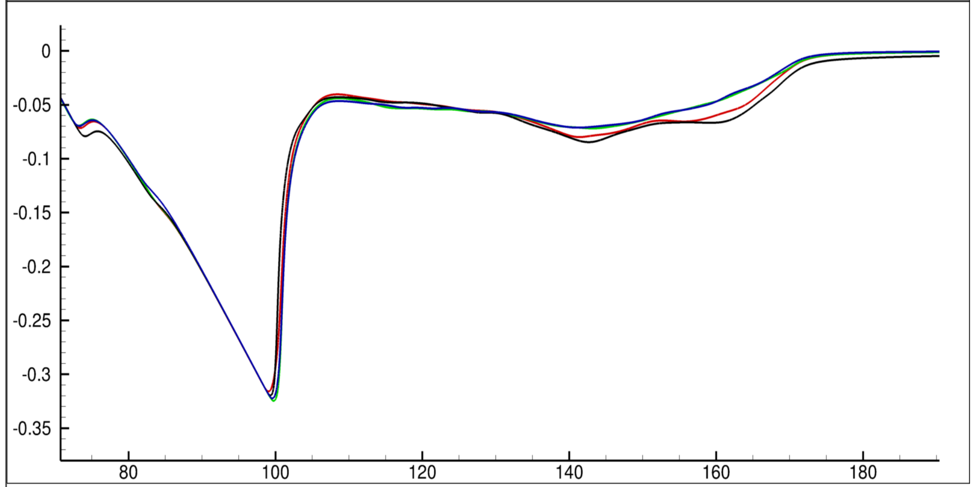

Left: Sonic boom ground signal; adjoint-adapted mesh predicts a closer loudness to fine mesh with significantly reduced cost

Top: Rise time signal comparison

Bottom: Pressure recovery signal comparison

Conclusion

- Demonstration of LAVA current toolset using the C608 and X-59
  - **Demonstrated ability to generate and run a given case in less than 8 hours**
  - Significant time savings compared to previous toolsets
- Space Marching
  - Enables factor of 2 savings over standard CFD approach with no loss in accuracy
- Database automation
  - Robust to changes in geometry, deflections, flight conditions
  - Demonstrated ability to meet LBFD milestone deliverable by completing database of 90 cases
  - Far less error prone
- Adjoint-based mesh redistribution
  - Eliminates manual off-body grid generation
  - Enables further factor of 2 savings for same accuracy
- Improvements to LAVA source code
  - Refactor of LAVA Unstructured improving speed and robustness
  - Curvilinear grid generation moving from OVERFLOW hole-cutting to LAVA hole-cutting, reducing wall time
- Glenn 8x6 wind tunnel comparisons
  - LAVA predictions are accurate and comparable to experimental results

Acknowledgments

- Work was funded by NASA's Commercial Supersonic Technology (CST) project and the Transformational Tools and Technologies (TTT) project
- Melissa Carter, Sriram Rallabhandi and the rest of the CST team for valuable technical discussions
- Daniel Maldonado, Ercan Dumlupinar, Michael Piotrowski for grid generation
- Brandon Lowe for assistance with adjoint solver development
- Members of the LAVA team from NASA Ames Research Center for valuable discussions
- Computer time has been provided by NASA's Advanced Supercomputing (NAS) at NASA Ames Research Center

References

- Jeffrey Housman, James Jensen, Gaetan Kenway, Cetin Kiris, "Efficient Near-Field to Mid-Field Sonic Boom Propagation Using a High-Order Space Marching Method", AIAA paper 2019-3487
- Jared Duensing, James Jensen, Jeffrey Housman, Michael Piotrowski, Daniel Maldonado, Emre Sozer, Cetin Kiris, Gaetan Kenway, "Structured and Unstructured Simulations for the Third AIAA Sonic Boom Prediction Workshop", AIAA Journal of Aircraft, 59(3): 1-23
- Jeffrey Housman, "Efficient Near-Field to Mid-Field Sonic Boom Propagation using a High-Order Space Marching Method", Advanced Modeling and Simulation (AMS) Seminar, August 13, 2019
- Jeffrey A. Housman, "Algorithmic Improvements to a High-Order Space Marching Method for Sonic Boom Propagation", Advanced Modeling and Simulation (AMS) Seminar, July 21, 2022
- Kiris et al, ”Computational framework for Launch, Ascent, and Vehicle Aerodynamics (LAVA)”, Aerospace Science and Technology 55
- Carter et al, “Experimental and Computational Study of the X-59 Wind Tunnel Model at Glenn Research Center 8- by 6-foot Supersonic Wind Tunnel”, NASA/TM–20220011496

Backup Slides

C608 Medium Grid Level Adaptation

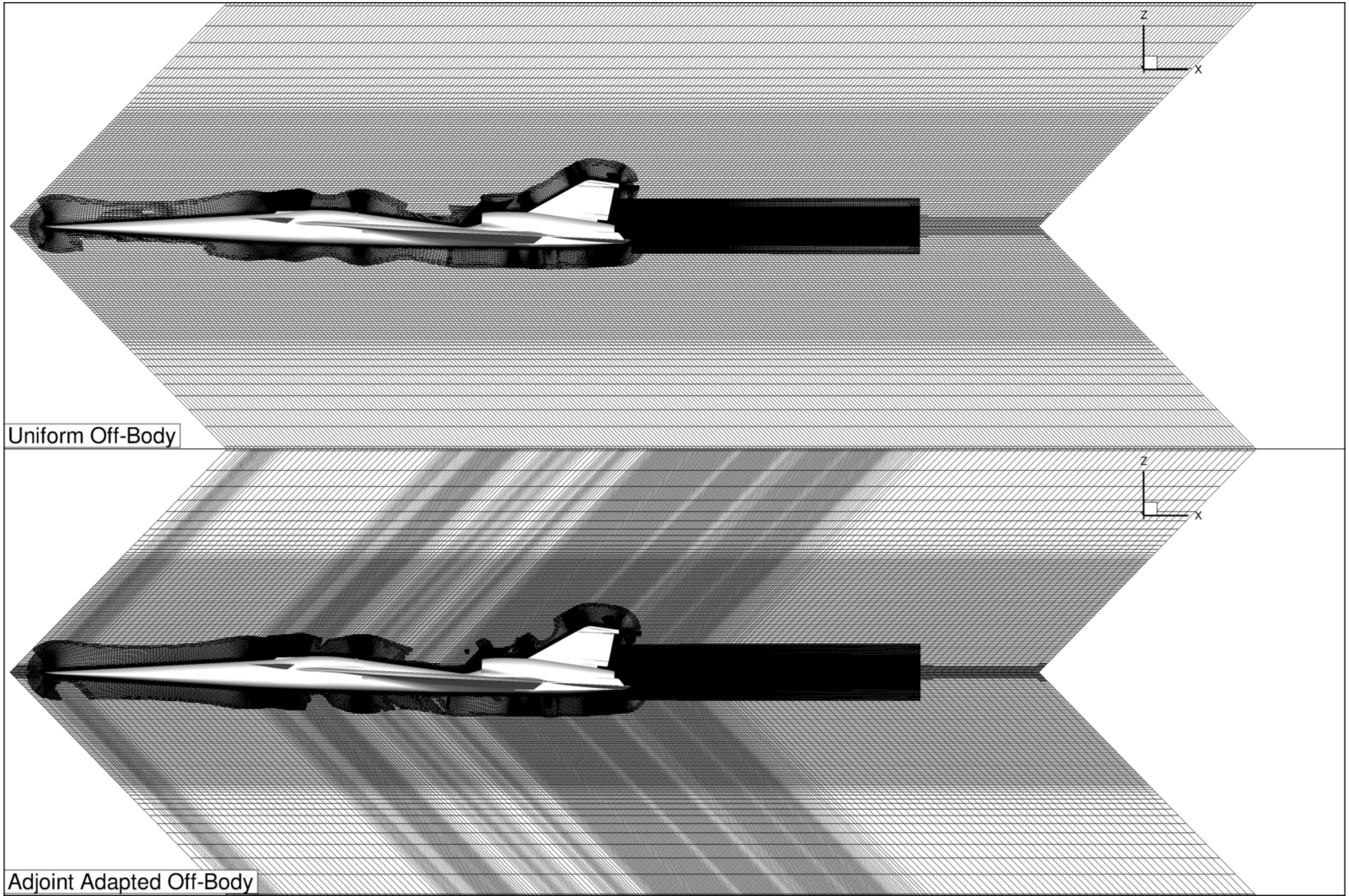

C608 : Adapted vs. Workshop Medium Grid Level

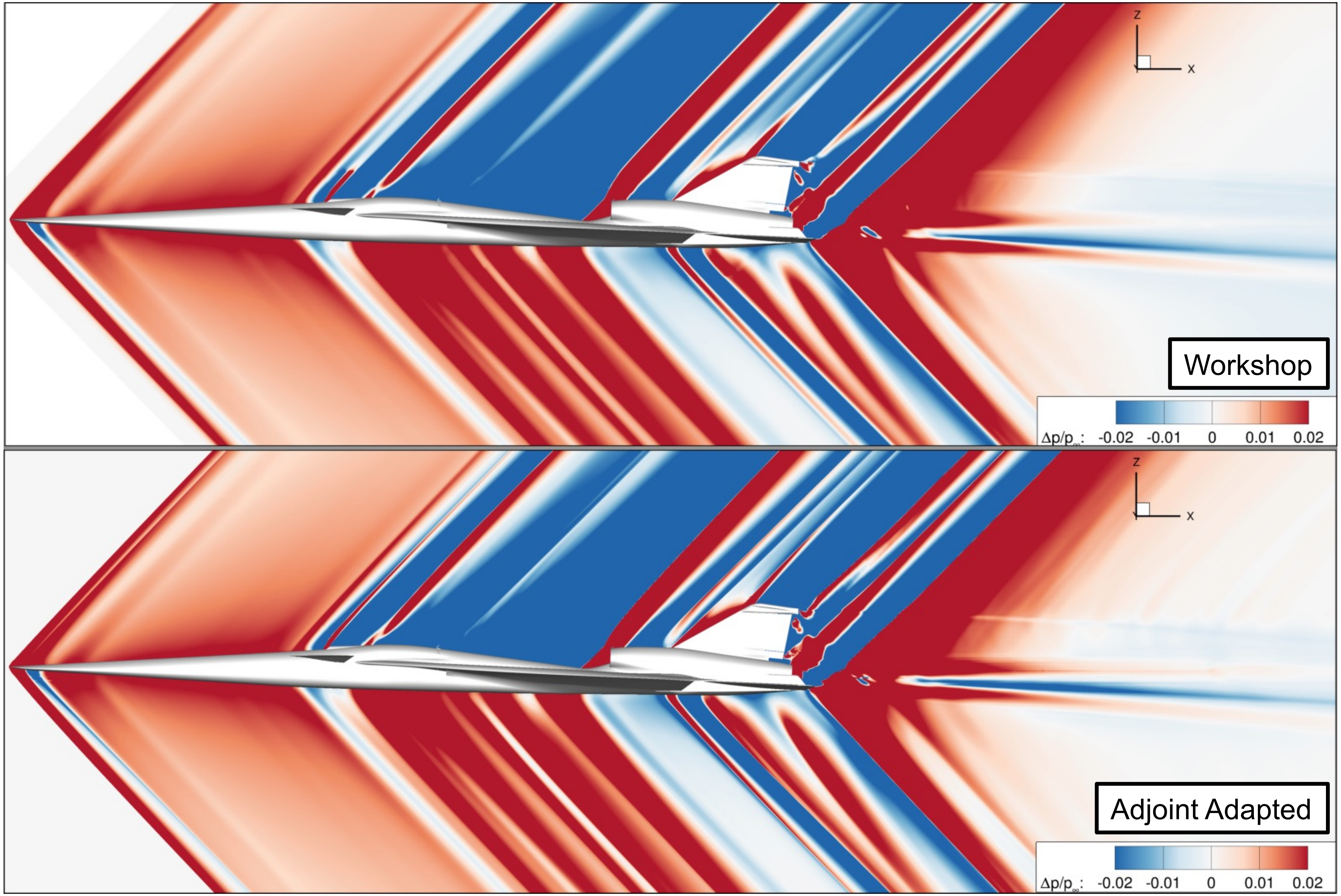

C608 : Adapted vs. Workshop Medium Grid Level

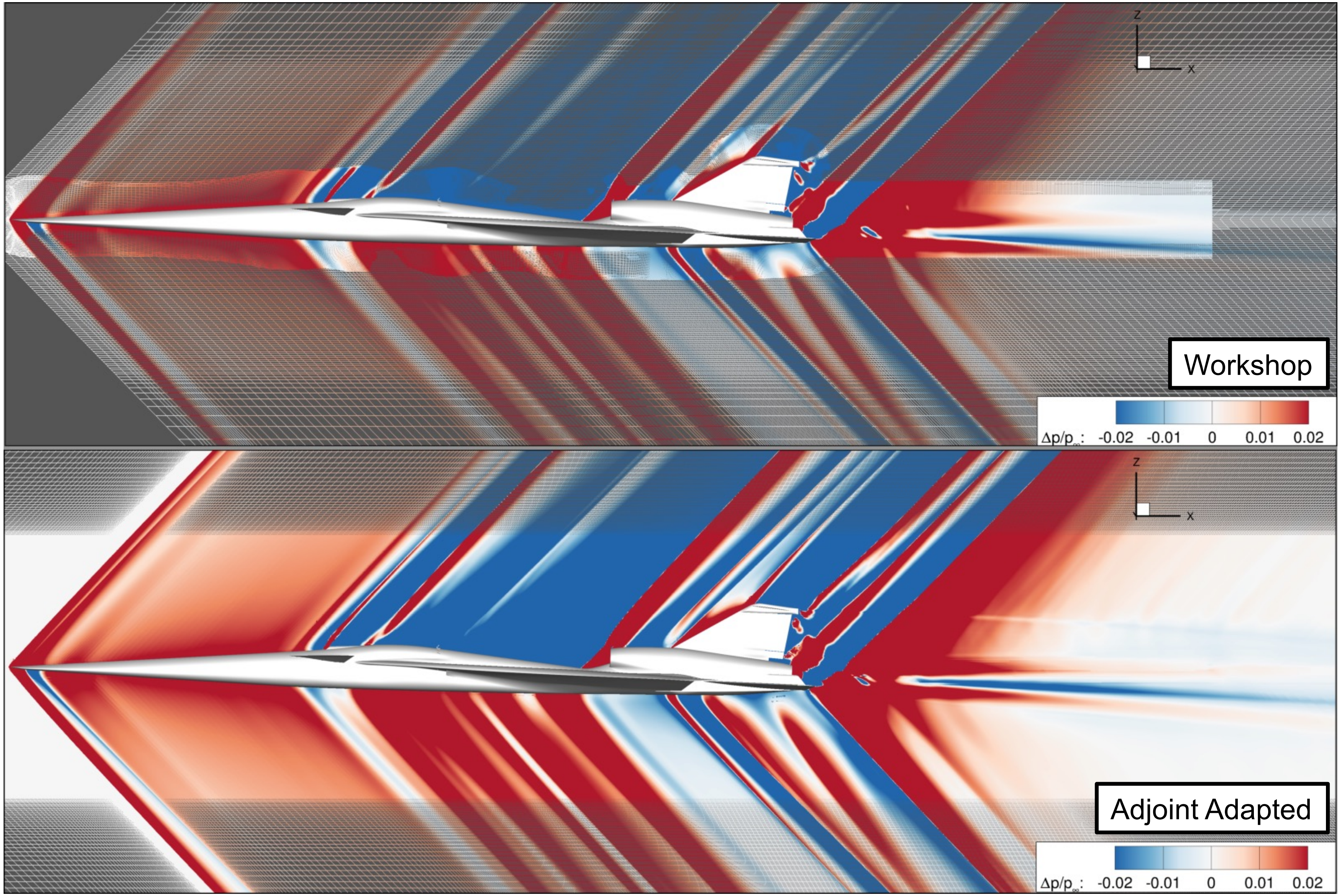

(From 2020) Improvements in the Structured Solver: CST Applications

- Ran Sonic Boom Prediction Workshop 3 Cases using both the old and refactored version of the structured solver and compared performance metrics
  - Comparisons shown here are all for the C608 geometry since it is more representative of the geometry that will be run for the X-59 database cases
- A representative case for future database runs will most likely sit between the medium and fine grid levels so the run costs are shown below
  - From these comparisons we expect to see a 3-5x speed-up
- Work on the refactored structured solver was jointly funded by TTT, CST, and AATT projects
  - Have shown a factor of speed-up of 9-12x for other applications (X-57)
- Met Milestone 331127: Curvilinear LAVA Code Optimization and Refactoring for LBFD Database Generation

	Old # CPUs	New #CPUs	Old Wall Time (hours)	New Wall Time (hours)
Medium	720	400	2.4	1.4
Fine	1500	1200	5.5	1.5

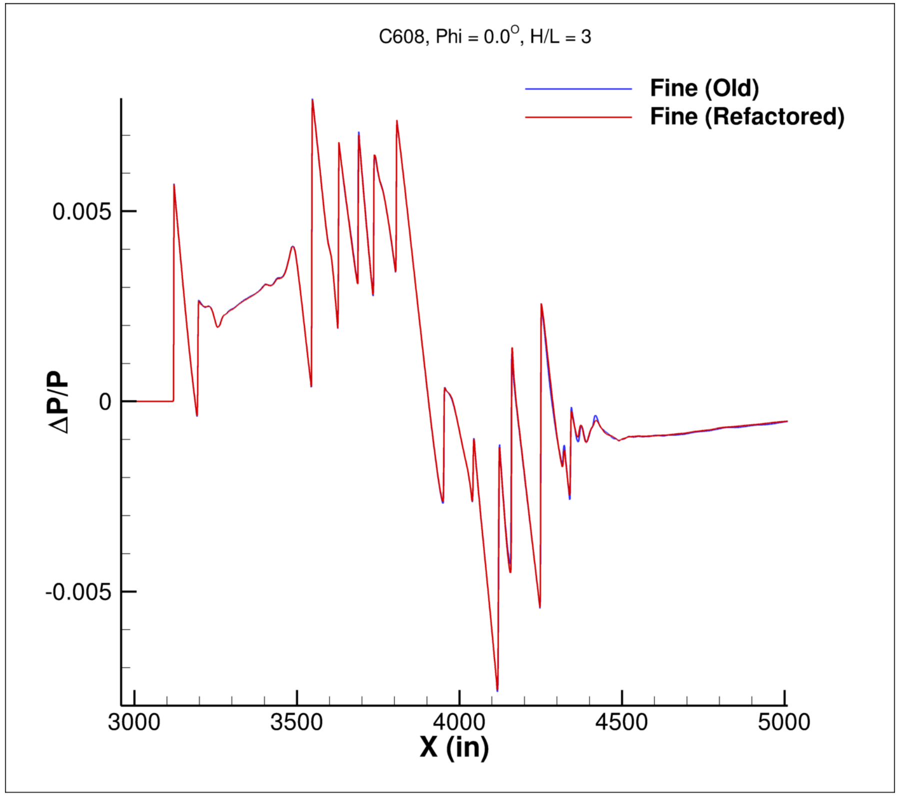

Case	Grid Level	Old SBU	Re-factored SBU	Improvement
C608	Coarse	18.15	6.36	2.85x
C608	Medium	57.8	18.3	3.16x
C608	Fine	274.0	59.4	4.60x